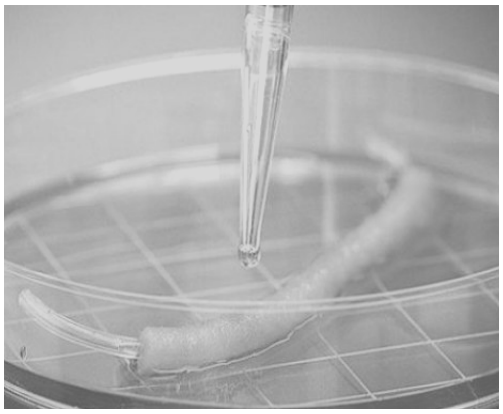

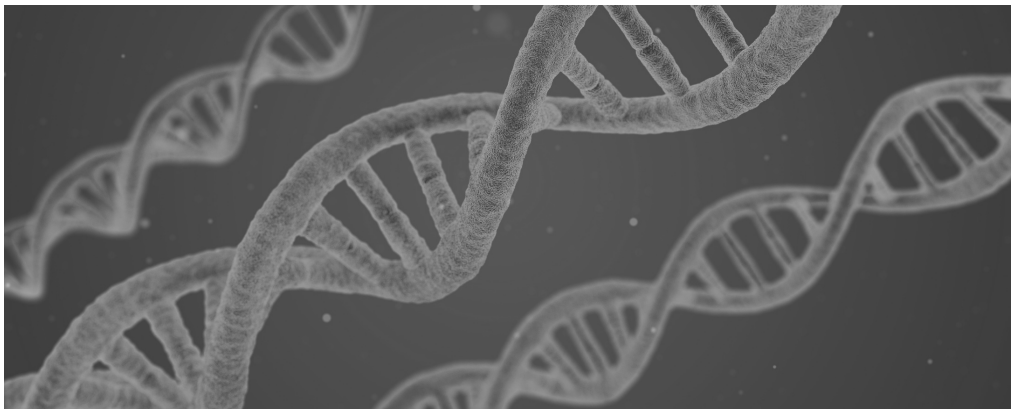

WELCOME TO THE THE INAUGURAL NORTHERN CALIFORNIA BIOMATERIALS DAY

EXPLORING THE NEXT HORIZON IN BIOMATERIALS RESEARCH

Friday 1.11.19

UC Davis Alumni Center

Society For Biomaterials
Giving life to a world of materials

UCDAVIS
BIOMEDICAL ENGINEERING

FRIDAY, JAN 11th, 2019

8:00am // Conference Opens, Coffee, Poster Setup, Check-in

8:30am // Conference Welcome, Prof. Kent Leach (UCD)

8:45am // Oral Session I

9:30am // Plenary Speaker, Prof. Niren Murthy (UCB)

10:00am // Coffee Break/Informal Poster Judging

10:15am // Keynote Address, Prof. David Grainger (University of Utah)

11:00am // Student Poster Session

12:00pm // Lunch

1:00pm // Industry Talk, Dr. Scott Kennedy (Verily Life Sciences)

1:30pm // Plenary Speaker, Prof. Sarah Heilshorn (Stanford)

2:00pm // Industry Career Panel (Dr. Scott Kennedy @ Verily; Dr. Kate Stuart @ Symic Bio; Drisha Leggitt @ Anpac Bio)

2:45pm // Coffee Break

3:00pm // Oral Session II

3:45pm // Awards Reception/Conference Closes

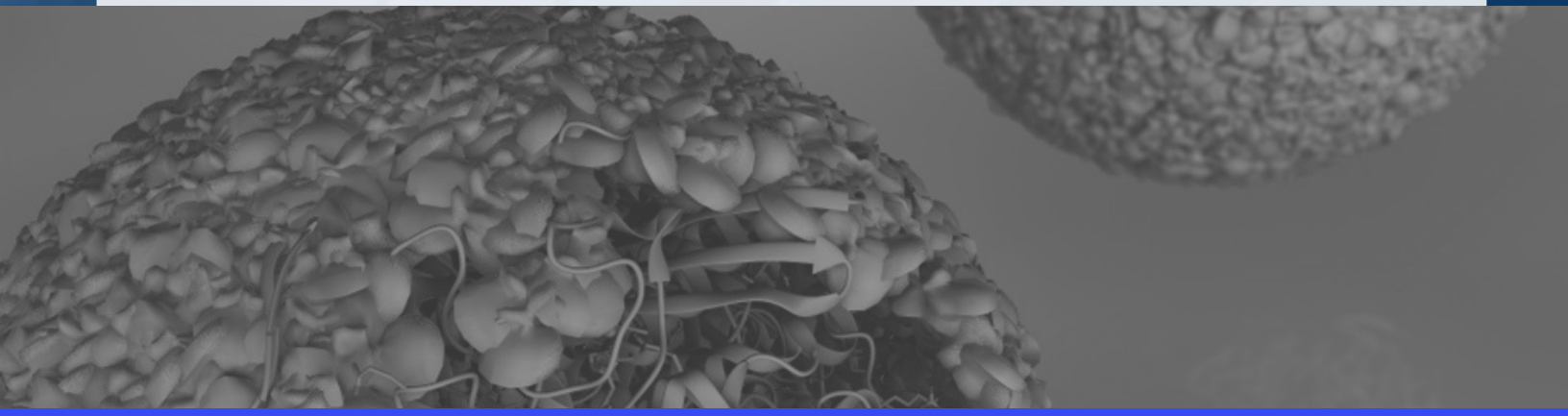

KEYNOTE SPEAKER

Prof. David Grainger

University of Utah

University Distinguished Professor and Chair, Department of Bioengineering
Distinguished Professor of Pharmaceutics and Pharmaceutical Chemistry
Adjunct Professor, Department of Orthopedics
Adjunct Professor, Department of Chemistry
Professor

Research Interests:

• Drug delivery systems and novel formulation strategies
• Polymeric biomaterials
• Antimicrobial medical devices, infection and bacterial colonization
• Nucleic acid and protein microarray diagnostics
• Macrophage interactions with biomaterials and the foreign body response
• Novel live vaccine and protein delivery
• Bioanalytical sensing and device miniaturization
• Surface analysis

Sarah Heilshorn

Stanford University

Associate Professor, Materials Science and Engineering
- Associate Professor (By courtesy), Chemical Engineering
- Associate Professor (By courtesy), Bioengineering

Bio: Heilshorn's interests include biomaterials in regenerative medicine, engineered proteins with novel assembly properties, microfluidics and photolithography of proteins, and synthesis of materials to influence stem cell differentiation. Current projects include tissue engineering for spinal cord and blood vessel regeneration, designing injectable materials for use in stem cell therapies, and the design of microfluidic devices to study the directed migration of cells (i.e., chemotaxis).

Prof. Niren Murthy

University of California, Berkeley

University Distinguished Professor and Chair, Department of Bioengineering

Professor in the Department of Bioengineering at the University of California at Berkeley

Research Interests:

Our laboratory is broadly focused on developing new molecules and materials for molecular imaging and drug delivery. Recent projects in the lab include the development of new probes for in vivo imaging of bacterial infections and reactive oxygen species. In addition, we also have a long standing interest in developing new materials for intracellular protein delivery.

INDUSTRY PANEL

Drisha Leggitt

Chief Marketing Officer

Anpac Bio

Ms. Leggitt is an internationally recognized public relations and marketing professional who has led marketing and PR nationally and internationally for major technology companies, including Hewlett-Packard, Agilent Technologies, and LCS Technologies. As a proud member of the Anpac Bio's leadership team, she leads partnership and investment development, communications and marketing, and external affairs. She enjoys applying her professional skills to educate the public and potential Anpac partners about Anpac Bio's cutting-edge Cancer Differentiation Analysis (CDA) technology, saving lives worldwide.

Anpac Bio-Medical Science Company, Ltd., is led by award-winning and internationally respected biomedical and nanotechnology scientists, research and medical professionals, engineering experts and physicists -- creating and launching break-through, leading edge, early cancer and other disease screening, detection, and diagnostic technology.

Dr. Kate Stuart

Senior Director Translational Biology

Symic Bio

Dr. Stuart has over 10 years of experience in research and development in the life science field, and is an inventor of Symic's core technology. After receiving a PhD degree in biomedical engineering from Purdue University, she continued at Purdue in a post-doc focused on early translation of the proteoglycan mimics. Previous to helping found Symic, Dr. Stuart worked in mid to late stage startup companies as a scientist and consultant on multiple marketed extracellular matrix technologies. She has served as PI on 5 small business grant awards.

Symic Bio is a biopharmaceutical company developing a new category of therapeutics focused on matrix biology. The (extracellular) matrix is the non-cellular component of the body's tissues and can be envisioned as a sponge-like environment surrounding the cells of a tissue. In this environment, cells proliferate, migrate and differentiate. Research in recent decades has demonstrated the biological importance of the interactive and dynamic relationship between cells and their matrix environment. The Symic Bio platform of matrix-targeting biotherapeutics builds upon this research. These therapeutics, inspired by naturally occurring macromolecules of the matrix called proteoglycans, bind to targets in the matrix damaged in response to injury or because of disease. They are designed to inhibit pathological inflammatory responses and to affect matrix degradation and structure.

Dr. Scott Kennedy

Verily Life Sciences (Alphabet Inc.)

Dr. Scott Kennedy is a research scientist at Verily Life Sciences (formerly Google Life Sciences). His research focuses on development of two types of smart contact lens devices: (1) a glucose sensing contact lens for diabetic patients and (2) an accommodating contact lens for people with presbyopia. He received his PhD in Polymer Science Engineering from University of Massachusetts, Amherst. Dr. Kennedy was a professor at Anderson University for nearly 13 years prior to joining Verily in 2014.

Verily aspires to create a world in which technology and life sciences are not distinct, but partners with a united mission. Formerly Google Life Sciences, Verily's mission is to bring together technology and life sciences to uncover new truths about health and disease. Verily's multidisciplinary teams have access to advanced research tools, large-scale computing power, and unique technical expertise. They work with partners from across the industry and many fields of research to develop new technology, launch studies, and start companies.

Student Oral Session I

8:45 AM **"Alginate Biomaterial Strategies for Potential Therapeutic Lymphangiogenic Applications"**
Kevin Campbell
UCD Biomedical Engineering

9:00 AM **"Development of fibrin:alginate interpenetrating networks for cell delivery"**
Charlotte Vorwald
UCD Biomedical Engineering

9:15 AM **"Compartments and Crowding: Biophysical Features of Living Cells"**
Wan-Chih Su
UCD Chemistry

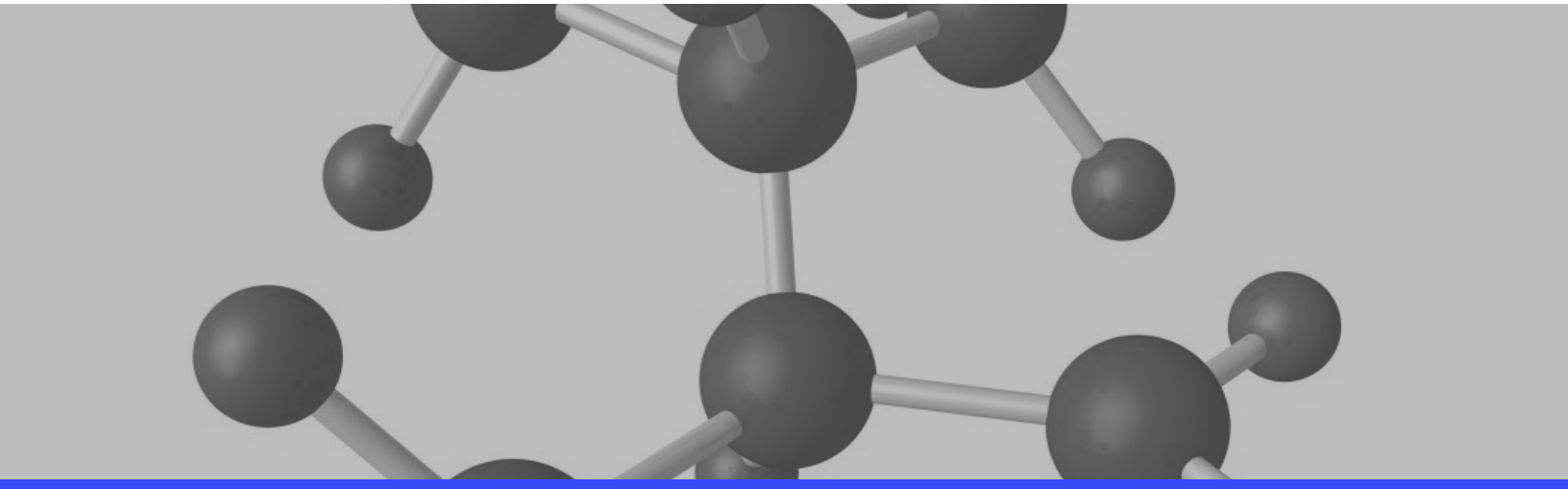

Student Oral Session II

3:00 PM **"Combining Nanoporous Metals and Single-Molecule Conductance for Sequence Specific Identification of Nucleic Acids in Complex Media"**

Jovana Veselinovic

UCD Chemical Engineering

3:15 PM **"Extracellular Matrix Enriched Spheroids for Enhanced Survival and Differentiation of Mesenchymal Stem Cells"**

Tomas Gonzalez-Fernandez

UCD Biomedical Engineering

3:30 PM **"Novel Extracellular Matrix Models to Study Dynamic Tissue Biomechanics"**

Juan A. Leal Doblado

CSU Los Angeles Physics

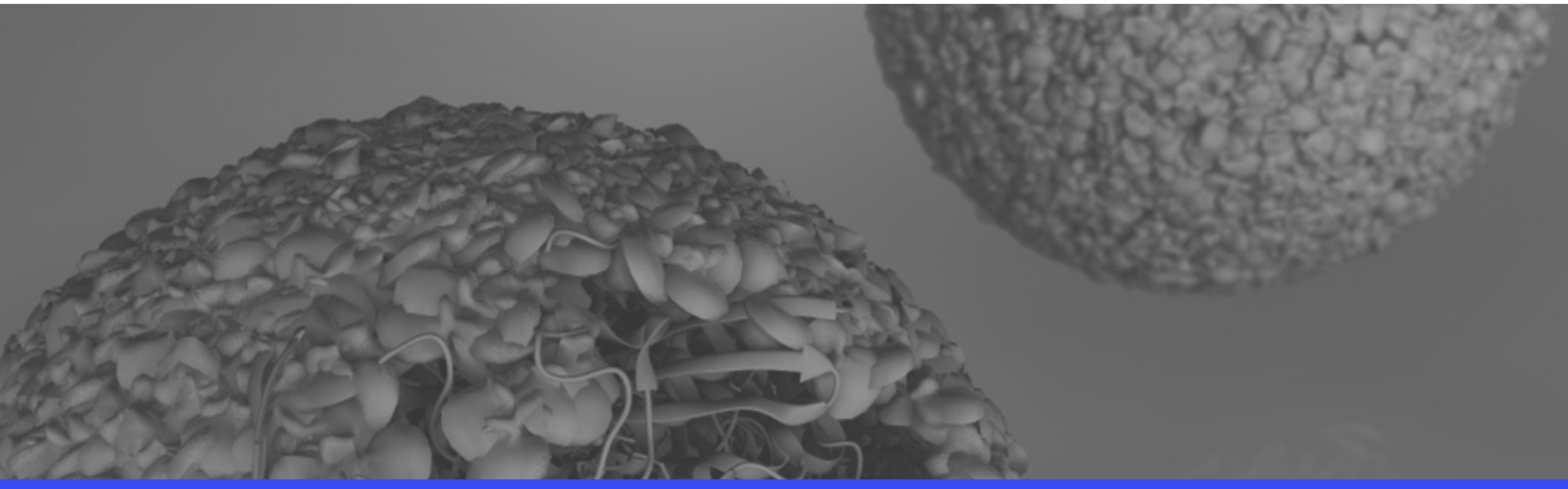

Poster Presentations

1. **"Injectable Dynamic Covalent Hydrogels of Boronic Acid Polymers Cross-Linked by Bioactive Plant-Derived Polyphenols"**
Peyman Delparastan
UCB Materials Science

2. **"Enzymatically Cross-linked Granular Support Material for Free-form Printing of Soft Materials"**
Gregory Girardi
UCD Biomedical Engineering

3. **"Core-Removal of Hollow Thermoresponsive Sub-Micron Particles for Cell Penetrating Peptide Delivery"**
Marcus Deloney
UCD Biomedical Engineering

4. **"Injectable Composite Hydrogels for Bone Repair in a Sheep Bone Defect Model"**
Marissa Gionet-Gonzales
UCD Biomedical Engineering

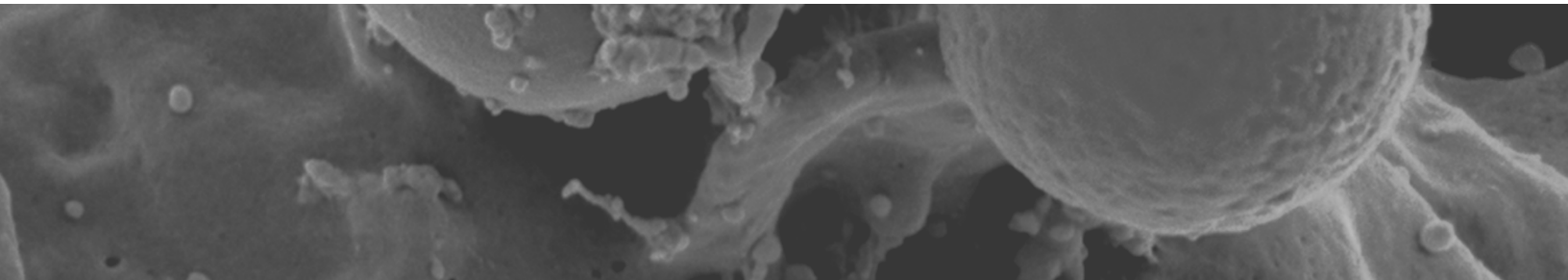

Poster Presentations

5. **"Trojan Horse nanotheranostics with dual transformability and multifunctionality for highly effective cancer treatment"**
Xiangdong Xue
UCD Physical Chemistry

6. **"Nanoporous Gold as a Multifunctional Neural Electrode Coating"**
Noah Goshi
UCD Biomedical Engineering

7. **"The Importance of Classical Elastica Theory in Microtubules Buckling"**
Fereshteh Memarian
UC Merced Physics

8. **"Development of an Exosome-mimic for Vascular Regeneration in Ischemic Wound Sites"**
Lalithasri Ramasubramanian
UCD Biomedical Engineering

Poster Presentations

9. **"Fabrication of Hydroxyapatite –Poly(lactide-co-glycolide) Composite Scaffolds with Reproducible Pore Geometry for Improved Cellular Infiltration and Alignment"**
Takeyah Campbell
UCD Biomedical Engineering

10. **"Selectin-targeting molecule acts as an antagonist to neutrophil adhesion and fibrosis"**
Tima Dehghani
UCD Biomedical Engineering

11. **"Thaw-Induced Gelation for the Encapsulation of Cryopreserved Cells in Alginate Capsules"**
Dustin J Hadley
UCD Biomedical Engineering

12. **"Characterizing the encapsulation and release of lentivectors and adeno-associated vectors from degradable alginate hydrogels"**
Shahin Shams
UCD Biomedical Engineering

Poster Presentations

13. **"Biophysical characterization of Bacteriorhodopsin entrapped in mesoporous silica gel monoliths"**
Sukriti Gakhar
UCD Chemical Engineering

14. **"Coupled flow and osmotic stress driven directed movement of vesicles"**
Sowmya Purushothaman
UCD Chemical Engineering and Material Science

15. **"Combinatorial, microparticle-based delivery of immune modulators reprograms dendritic cell phenotype and promotes remission of collagen-induced arthritis in mice"**
Riley Allen
UCD Biomedical Engineering

16. **"Environment-Responsive Two-Fluorophore Reporter System: A Potential Tool to Monitor Particulate Vomocytosis"**
Noah Pacifici
UCD Biomedical Engineering

Poster Presentations

17. **"Towards a Nanoparticle-based Prophylactic for Maternal Autoantibody-related Autism"**

Amir Bolandparvaz

UCD Biomedical Engineering

Special Thanks to the Organizing Committee, Society for Biomaterials, and UC Davis Biomedical Engineering for their generous support.

Society For Biomaterials

Giving life to a world of materials

UCDAVIS BIOMEDICAL ENGINEERING

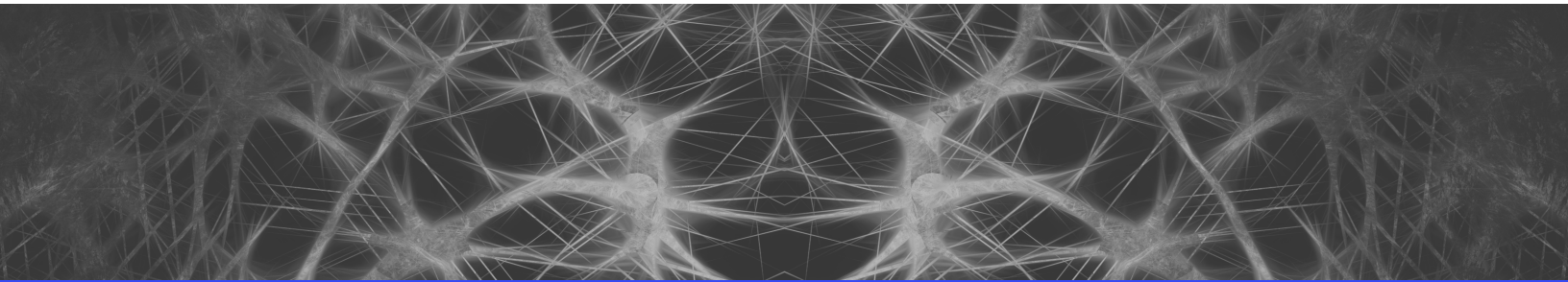

Visitor Information

Electric Vehicle Charging
Station Information

4 hour limit on all charging stations.

.

Posted parking restrictions apply in EV charging locations.

.

ChargePoint Chargers are compatible with both 110 volt vehicles.

.

Units may be activated with a ChargePoint card or bank issued credit card (VISA, Mastercard, Discover)

.

Clipper Creek chargers are equipped with SAE J-1772

Alginate Biomaterial Strategies for Potential Therapeutic Lymphangiogenic Applications

Kevin Campbell, Dustin Hadley, Roberta Stilhano, Dave Kukis and Eduardo Silva.
Department of Biomedical Engineering, University of California, Davis.

Purpose: The lymphatic system is essential for tissue regeneration due to its pivotal role in maintaining tissue homeostasis. Loss of functional lymphatic vasculature has been implicated in the pathogenesis of several cardiovascular disorders including obesity, inflammation, atherosclerosis, hypertension and myocardial infarction. Stimulating new lymphatic vessels (lymphangiogenesis) has recently attracted attention as a promising strategy to reverse the progression of these diseases. In particular, two promising approaches for stimulating lymphangiogenesis involve the delivery of vascular endothelial growth factor (VEGF) members VEGF-C and VEGF-D or endothelial progenitor cells (EPCs), which contain both blood and lymphatic subpopulations that promote neovascularization. However, challenges in maintaining spatial and temporal presentation of these factors and lack of control of cell fate *in vivo* limits their current applications. Thus, this work tested the utility of injectable and degradable alginate hydrogels for 1) providing sustained and bioactive release of VEGF-C and VEGF-D and for 2) delivering and attenuating EPC migration for potential therapeutic applications.

Methods: For growth factor release studies, alginate hydrogels were loaded with radiolabeled VEGF-C and VEGF-D to determine the release kinetics of both growth factors. Bioactivity of alginate released growth factors were assessed with their ability to promote human microvasculature lymphatic endothelial cell (LEC) sprouts in 3D sprouting assays and promote increased vasculature density *in vivo* via a chick chorioallontoic (CAM) assay. For EPC delivery studies, alginate hydrogels were loaded with various concentrations of alginate lyase (AL), an enzyme which cleaves alginate polymers, to assess hydrogel degradation and mechanical properties over three weeks. Finally, the ability of delivered cells to promote new vasculature was tested *in vivo* via a CAM assay.

Results: LECs were sensitive to the temporal presentation of both VEGF-C and VEGF-D and both radiolabeled growth factors experienced continuous release from alginate hydrogels over the course of a week. Alginate delivered VEGF-C and VEGF-D promoted LEC sprouts *in vitro* and new vasculature *in vivo*. Additionally, higher concentrations of AL incorporated into alginate hydrogels mediated degradation, loss of storage modulus and led to significant increases in mesh size over time. Hydrogels with EPCs and AL were also able to promote cell migration *in vitro* and increased vasculature and perfusion *in vivo* (figure 1).

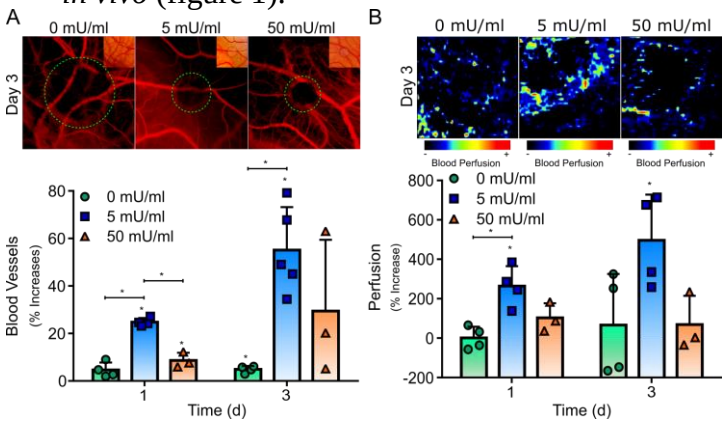

Figure 1. Hydrogels incorporating EPCs and 5 mU/ml of AL promoted significant increases in vasculature density (A) and perfusion (B) in a CAM assay. Asterisk indicates $P < 0.05$.

Conclusions: This study investigates the use of injectable and degradable alginate hydrogels to deliver growth factors and cell based therapies for potential future lymphangiogenic therapeutic applications. This work determined that alginate hydrogels provided sustained and bioactive release of VEGF-C and VEGF-D. Furthermore, enzymatically degradable alginate hydrogels allowed for control over various mechanical properties of the hydrogels which altered the migration of encapsulated EPCs and promoted new functional vasculature *in vivo* via a CAM assay. Overall, this is the first study characterizing VEGF-C and VEGF-D release from alginate hydrogels and the use of AL to mediate EPC delivery for potential lymphangiogenic applications.

Development of fibrin:alginate interpenetrating networks for cell delivery

Charlotte Vorwald[a], Pawel Sikorski[a,b], Tomas Gonzalez-Fernandez[a], Shreeya Joshee[a], and Kent Leach[a,c]
[a]Department of Biomedical Engineering, University of California, Davis, Davis, CA
[b]Department of Physics, Norwegian University of Science and Technology, Trondheim, Norway
[c]Department of Orthopaedic Surgery, UC Davis Health, Sacramento, CA

Statement of Purpose: Tissue engineering seeks to provide cell-instructive cues for tissue regeneration and to ultimately speed healing in compromised wounds. Cell-based strategies are an exciting opportunity to promote neovascularization, wound healing, and tissue repair, but cell viability and function upon implantation remain a critical challenge. Co-culture cell transplantation using proangiogenic mesenchymal stem cells (MSCs) and vessel-forming endothelial colony forming cells (ECFCs) is pursued to synergistically promote neovascularization and tissue formation. A suitable scaffold carrier that allows both compliance for vascularization and mechanical properties conducive for cell invasion or differentiation is essential for successful deployment. Utilizing an interpenetrating network (IPN) composed of two natural polymers, fibrin and alginate, we can tune the structural and morphological characteristics of such carriers to influence vascular network formation and stem cell fate. The overall objective of this study is to synergistically combine the structure of fibrin, which is beneficial for cell infiltration, and the tunable biophysical properties of alginate to cooperatively influence the function of entrapped co-cultures for tissue repair.

Methods: We evaluated construct morphology to create a uniform fibrin:alginate IPN (FA IPN) with dense fibrin structure. FA IPNs (10 mg/mL fibrinogen and 2% w/v oxidized alginate) were fabricated with varying concentrations of thrombin (0.025, 0.05, 0.25, and 0.5 U/mL) to assess fibrin morphology and structure *via* light reflection confocal microscopy. We encapsulated co-cultures at a 1:1 ratio of MSCs to ECFCs in FA IPNs (0.25 U/mL thrombin) for continuous culture in mixed cell growth medium. We performed confocal microscopy on Day 0, 1, 3, and 7 to assess cell network formation. Homogenous fibrin and alginate constructs served as positive and negative controls, respectively.

Results: We successfully fabricated FA IPNs with varying concentrations of thrombin **(Fig. 1 A)** to yield constructs with distinct fibrin structures within pre-crosslinked alginate solutions **(Fig. 1B)**. Within 3 days of continuous culture, entrapped co-cultures in FA IPNs created robust networks that were comparable to fibrin positive controls **(Fig. 1C)**.

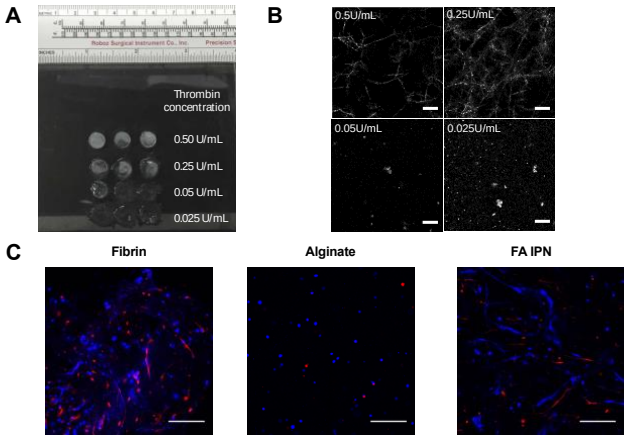

Figure 1. (A) Gross morphological image of FA IPNs formed after 30 min of gelation. **(B)** Light reflection confocal microscopy images of FA IPNs fabricated with varying concentrations of thrombin. Scale bars are 10 μm. **(C)** Confocal images of 1:1 ECFC:MSC FA IPNs on Day 3 of culture. ECFCs are violet and MSCs are red. Scale bars are 250 μm.

Conclusion: These findings demonstrate a novel hydrogel carrier with desired structural and morphological properties that can influence entrapped cells when used for tissue engineering applications. Future work will assess mechanical properties of these formulations and investigate the ability of these materials to instruct MSC differentiation while enabling network formation.

Compartments and Crowding: Biophysical Features of Living Cells

A central objective of my research is to determine how macromolecular crowding, which characterizes the cytoplasmic milieu of living cells, affects cellular response to osmotic stress. My research strategy is to develop and deploy a carefully selected set of well-characterized vesicular model systems, which recapitulate the essential physical features of living cells including femtoliter scale compartmentalization of the aqueous phase; molecular crowding and phase separation within the cellular interior; and compositionally diverse, and structurally elastic, membrane boundary. These models will then be used to generate quantitative relationships, which map (1) the model protocells that reconstitute "macromolecular crowding" inside; (2) mesoscale shape transitions in ATPS-encapsulating giant vesicles subject to osmotic gradients; and (3) the compositional dependence (i.e., domain formation) of ATPS-encapsulating giant vesicles.

The interior of a living cell is packed with large macromolecules (e.g., nucleic acids, proteins and polysaccharides), cytoskeletal filaments, and organelles. Furthermore, this physical crowding in the cellular cytoplasm is highly dynamic continually changing the diffusional properties of embedded solutes, molecular (and ionic) concentration gradients, and phase separation or dynamic micro-compartmentalization of the cytosolic fluid. But how this cytoplasmic macromolecular crowding and accompanying dynamic micro-compartmentation affects membrane shapes and molecular organization?

Building on the experimental model system developed by Keating (PNAS, 2005), Dimova, and Lipowsky (Soft Mattter, 2012), we reconstitute minimal crowding and conditions for dynamic microcompartmentation inside cell-sized giant vesicles. Specifically, we encapsulate a uniform aqueous phase mixture of two water soluble polymers (namely, dextran and poly(ethylene)glycol), which when subject to osmotic deflation, assumes relative concentrations that produce aqueous two-phase separation (ATPS) in real-time. We find that the onset of vesicular micro-compartmentation in the encapsulated aqueous phase is accompanied by an active membrane remodeling inducing vesicle morphogenesis. Unlike equilibrium configurations, we find that multiple buds of essentially uniform size decorate the membrane boundary reflecting a competition between phase coarsening dynamics during the spinodal decomposition of the ATPS and preferential wetting of the membrane surface by the dextran-rich phase. Our results suggest the stabilization of a rich variety of membrane morphologies through kinetically determined membrane deformation processes, far exceeding the narrow range of shapes obtained under thermodynamic equilibrium.

Title: Combining Nanoporous Metals and Single-Molecule Conductance for Sequence Specific Identification of Nucleic Acids in Complex Media

Co-authors: Mashari N. Alangari, Zimple Matharu, Yuanhui Li, Joshua Hihath, Erkin Seker; Department of Electrical and Computer Engineering, University of California, Davis, CA, 95616

Purpose: Nucleic acid-based biosensors have enabled rapid and sensitive detection of pathogenic targets; however, these devices often require purified nucleic acids for analysis since the constituents of complex biological fluids adversely affect sensor performance. In addition, sensors capable of detecting not only the presence of specific nucleic acids in complex media, but their polymorphisms as well, are required for the routine screening of genetic mutations and diseases. We report a two-tiered platform consisting of a multifunctional matrix, nanoporous gold (np-Au) and single-molecule conductance measurements that can electrically detect, purify, and distinguishing mismatched nucleic acid sequences (DNA and RNA) in complex biological liquid samples.

Methods: The first tier of the platform uses a nanoporous gold (np-Au) for the electrochemical detection and subsequent purification of nucleic acids. Nanoporous gold (np-Au) electrode coatings produced by alloy corrosion process have played significant role in enhancing the performance of electrochemical nucleic acid biosensors owing to their three-dimensional nanoscale network of pores and ligaments, electrical conductivity, facile surface functionalization, and biocompatibility. In this study, np-Au electrodes were modified with 15-mer DNA probes (via thiol-gold chemistry). Upon target capture using immobilized probes, the non-complementary DNA fragments and complex media constituents of varying sizes were washed away. Finally, the surface-bound DNA:DNA or DNA:RNA duplexes were released by electrochemically cleaving the thiol−gold linkage, eluting the hybrids from the nanoporous matrix for further analysis in the second tier of our platform. The second tier uses electrical conductance measurements to verify sequence information and identify the presence of mismatches between the DNA probe and the RNA target. This step utilizes the single-molecule break junction (SMBJ) to measure samples eluted from the first-tier to reduce the possibility of false positives from similar target sequences. Two-tiered approach was applied to detect a 15-base pair (bp) *E. coli*. RNA sequence spiked in blood, and was further expanded to differentiate between the perfectly-matched case and partial mismatches of the RNA:DNA hybrids.

Results & Discussion: The platform was first validated for the biofouling-resilience of np-Au in detecting RNA spiked in complex media. The sieve-like structure of np-Au blocks the permeation of large biomolecules and allows for selective transport of nucleic acids to the sensing surface, thereby obviating the need for prior purification steps. We have demonstrated that np-Au allows for the detection of 15-base pair (bp) *E. coli*. RNA sequence spiked in blood, for both perfectly-matched and partially mismatched RNA:DNA hybrids, by observing change in the electrochemical current signal before and after the hybridization event. Complementary to the electrochemical screening approach, single molecule conductance measurements provided a molecular insight that is unavailable using electrochemical methods, by measuring the magnitude of the current passing through the molecule which changes drastically in the case of a mismatched hybrid. We were able to differentiate between perfectly matched versus mutated targets (3-base mismatch) found in the eluted sample from the first stage, through the observed differences in the conductance fingerprint.

Conclusion: In this study we were able to purify and detect both, perfectly and partially matched, 15-merDNA:RNA hybrids from whole blood. This multifunctional platform is expected to enable seamless integration of detection and purification of nucleic acid biomarkers of pathogens and diseases in miniaturized diagnostic devices for point-of-care applications.

Extracellular Matrix Enriched Spheroids for Enhanced Survival and Differentiation of Mesenchymal Stem Cells

Tomas Gonzalez-Fernandez[1], Andrew T. Keown[1], Alejandro J. Tenorio[1], J. Kent Leach[1,2]
[1]Department of Biomedical Engineering, University of California, Davis, Davis, California 95616, USA
[2]Department of Orthopaedic Surgery, School of Medicine, UC Davis Medical Center, Sacramento, California 95817, USA

Statement of Purpose: The recapitulation of the cellular niche is of special importance to promote stem cell survival and phenotype specification following transplantation. The formation of mesenchymal stem cells (MSCs) into three-dimensional spheroids enhances their survival, trophic factor secretion, and tissue-forming potential compared to monodisperse cells (1). Moreover, cell-secreted ECM represents a more complex platform to recapitulate the cues to guide stem cell fate versus individual matrix proteins or functional motifs (2). We previously demonstrated that MSC-secreted ECM increased progenitor cell osteogenic differentiation of diverse origins and donor populations (2). Therefore, we hypothesized that the formation of MSC spheroids enriched with cell-secreted ECM would enhance MSC viability, proliferation and differentiation potential.

Methods: Commercially available human bone marrow-derived MSCs were expanded *in vitro* until passage 4 and then either formed into spheroids as previously described (1) or used in monolayer culture for ECM production following a previous protocol (2). After lyophilization, MSC-secreted ECM was incorporated into MSC spheroids. Incorporation efficiency was confirmed through biochemical and histological assays, environmental scanning electron microscopy (ESEM), and measurement of spheroid diameter. MSC morphology in the ECM-loaded spheroids was analyzed by fluorescent imaging of the actin cytoskeleton. Cell viability was assessed through DNA and cell metabolic activity quantification and live/dead staining. The differentiation of MSCs towards the chondrogenic and osteogenic phenotype within ECM-loaded spheroids was assessed through biochemical and histological analysis of calcium, sulfated glycosaminoglycans (sGAG) and collagen deposition after 21 days of *in vitro* culture in conditioned media.

Results: MSC spheroids formed with exogenous MSC-secreted ECM possessed larger spheroid diameters (Fig. 1A), increased cell viability (Fig. 1C) and higher collagen (Fig. 1D) and sGAG (Fig.1E) content as the concentration of ECM increased from 0 to 7.5 µg of ECM per spheroid. The fluorescent assessment of cell morphology (Fig. 1B) revealed expanded cell cytoskeleton and higher separation between cell nuclei with the addition of ECM. To test the differentiation potential and MSC response in the presence of ECM, MSC spheroids enriched with 5 µg of ECM were cultured for 21 days in growth, chondrogenic, or osteogenic media and compared to non-enriched spheroids and spheroids enriched with 5 µg of type I collagen. ECM-laden MSC spheroids exhibited significantly higher levels of DNA (Fig. 1F), collagen (Fig. 1G) and sGAG (Fig. 1H) content in all media conditions compared to control and collagen-laden spheroids. In addition, ECM-enriched spheroids in osteogenic media possessed a highly mineralized matrix that confirmed effective osteogenic induction.

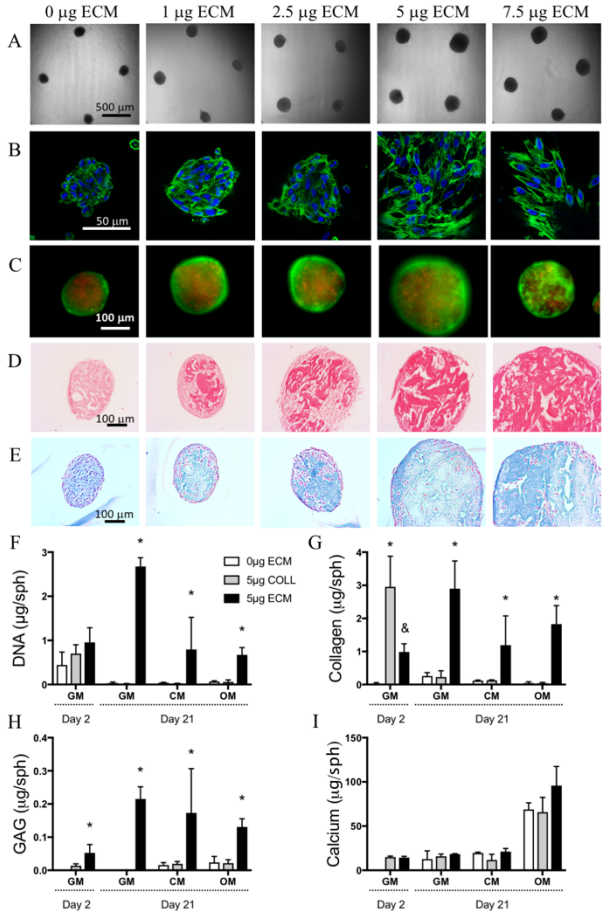

Figure 1. (A) Brightfield images of MSC spheroids enriched with 0, 1, 2.5, 5 and 7.5 µg of ECM per spheroid after 48h of formation. (B) Fluorescent imaging of the MSC cytoskeleton (green) and nucleus (blue) of MSCs within the spheroids. Live/dead (C), collagen (D) and sGAG (E) staining of the spheroids. Quantification of DNA (F), collagen (G), sGAG (H) and calcium (I) content of the non-enriched (0 µg ECM), collagen and ECM-enriched spheroids after 21 days of culture in growth (GM), chondrogenic (CM) or osteogenic (OM) media. * Indicates statistical significance versus other groups in same media ($p<0.05$).

Conclusions: The tailoring of the MSC 3D environment through the incorporation of ECM into MSC spheroids is a promising approach for the instruction of stem cell phenotype and function. The addition of ECM to MSC spheroids enhanced MSC response to soluble cues, providing an opportunity to enhance their therapeutic potential in tissue engineering applications.

References: (1) Ho SS. Stem Cells 2018,36(9):1393-1403, (2) Harvestine JN. J. Mater. Chem. B 2018,6:4104-4115.

Title: Novel Extracellular Matrix Models to Study Dynamic Tissue Biomechanics

Purpose: Pancreatic cancer is difficult to diagnose because the pancreas is deep inside the body, making early tumor detection difficult. While this disease causes changes in the extracellular matrix (ECM) of pancreatic tissue, noninvasive diagnostic tools to detect these changes are lacking because little is known about how these changes affect biomechanical characteristics. Studying the mechanics of living tissue is a challenge due to the complex viscoelastic behavior of biological samples and the limitations of current biomechanical models. An optical fiber polarimetric elastography (OFPE) device was developed to overcome these limitations. OFPE allows for high resolution mechanical testing, which allows us to capture the global mechanics of the ECM. Additionally, to validate the experimental results obtained during OFPE compressing testing, we designed and fabricated 3D printed biomimetic structures of pancreatic tissue, and modeled their mechanical behavior using finite element analysis (FEA),

Methods:

Compressive Testing: Pancreatic tissue samples were tested using the OFPE device. Due to its unique structure, the biomimetic structures were tested using an Instron Loadframe. Strains of 10%, 20%, and 30% were applied to each sample over 30 s loading and unloading intervals.

Biomimetic Structure Design and Computer Modeling: Using previous pancreatic imaging studies as a template, we computationally modeled simple geometric lattices in SolidWorks. Ten geometric variants of the base structure were designed, five of which, had varying diameter to length (D/L) ratios. The remaining five structures had different support beams removed.

Biomimetic Structure Fabrication: The biomimetic structures were fabricated using projection microstereolithography.

FEA Modeling: FEA modeling was carried out using Abaqus FEA. Using the neo-Hookean material model, we are able to model the structures' response to compressive loading.

Results: The results from compressive testing of the pancreatic tissue using the OFPE device showed that the buckling point is between 22 and 25% strain. These results are supported by the effects of compressive testing of the biomimetic structure. In particular, the design missing two adjacent support beams revealed that it had buckling characteristics that were experimentally similar to that of pancreatic tissue. Using FEA modeling results of the biomimetic structures, we determined that the buckling point is linearly correlated to the D/L ratio.

Conclusion: Biomimetic structures can be used to complement and identify the microstructures of biological tissues that are analyzed via OPFE. We identified collagen IV as the predominant pancreatic microstructural ECM component most similar to the system modeled using the linear fit as a calibration curve. Thus, by focusing on the geometric changes that result from a diseased state, these models can provide accurate insights into the biomechanics of pancreatic tissue. In the future, these models can be used to study the mechanics of other tissues, including cardiac tissue.

Injectable Dynamic Covalent Hydrogels of Boronic Acid Polymers Cross-Linked by Bioactive Plant-Derived Polyphenols

Zhuojun Huang,[a] Peyman Delparastan,[a] Patrick Burch,[a] Jing Cheng,[a] Yi Cao,[c] and Phillip B. Messersmith [a,b]

a) Departments of Bioengineering and Materials Science and Engineering, University of California, Berkeley, CA, US

b) Materials Science Division, Lawrence Berkeley National Laboratory, Berkeley, CA, US

c) Department of Physics, Nanjing University, Nanjing, China PR

Statement of Purpose: Plant polyphenols are a family of naturally derived compounds that contain a high concentration of phenolic hydroxyl groups. These molecules are linked to diverse biological functions and are highly celebrated for their complex bioactivities and antioxidant behavior. A high dietary intake of polyphenols has been linked to a reduced incidence of a number of diseases, including cancer, diabetes, osteoporosis as well as cardiovascular and neurodegenerative diseases, and several polyphenols have been investigated as therapeutics. However, despite their impressive therapeutic effects, polyphenols suffer from a number of drawbacks which limit their clinical translation, including poor bioavailability, rapid metabolism, and poor membrane permeability. Therefore, development of an efficient delivery method for these beneficial therapeutic molecules would be a milestone in translation into the clinic. The high hydroxyl content and rich bioactivity spectrum of polyphenols presents a unique opportunity to form therapeutically active dynamic covalent hydrogels with boronic acid polymers. Herein we exploit the pH dependence and dynamic nature of complexes between boronic acid functionalized PEG and polyphenols as bioactive injectable hydrogels (**Figure 1**). In this concept, the polyphenol functions both as cross-linker and therapeutic, forming a hydrogel by injection of a precursor solution of polymer and polyphenol that solidifies through formation of boronate ester cross-links upon neutralization to physiologic pH. The dynamic nature of the boronate ester bond provides a mechanism for latent hydrogel disassembly and release of therapeutic polyphenols into the surrounding environment.

Methods: A modular approach was adopted whereby PEGs of different molecular weights and architectures were functionalized with four different phenylboronic acids (BAs) with pK_a values ranging from 6.9 to 9.0. Numerous combinations of natural polyphenols, PEG-BA polymers of different architecture were screened by rheological analysis, revealing several formulations that gave rise to rapid gelation at physiologic pH. Insight into the molecular mechanics of boronic acid-polyphenol interactions was provided by measuring bond rupture forces in a pH dependent manner using single molecule force spectroscopy (SMFS). Finally, we studied the kinetics of EA release from a PEG-boronic acid hydrogel and demonstrated the *in vitro* cytotoxic effects of released EA on cancer cells.

Results: We report the development of hydrogels formed at physiological conditions using PEG based polymers modified with boronic acids as backbones and the plant derived polyphenols ellagic acid (EA), epigallocatechin gallate (EGCG), tannic acid (TA), nordihydroguaiaretic acid (NDGA), rutin trihydrate (RT), rosmarinic acid (RA) and carminic acid (CA) as linkers. The influence of polymer architecture and boronic acid pK_a was revealed using EGCG as a model cross-linker showing expected trends in hydrogel stability when the pK_a value of boronic acid is changed. Rheological frequency sweep and single molecule force spectroscopy (SMFS) experiments show that hydrogels linked with EGCG and TA are mechanically stiff, arising from the dynamic covalent bond formed by the polyphenol linker and boronic acid functionalized polymer. Stability tests of the hydrogels in physiological conditions revealed that gels linked with EA, EGCG, and TA are stable for more than two months in excess buffer, while gels formed with other linkers were completely dissolved over the course of several days. We furthermore showed that EA- and EGCG-linked hydrogels can be formed via *in situ* gelation in pH 7.4 buffer, and provide long-term steady state release of bioactive EA. *In vitro* experiments showed that EA-linked hydrogel significantly reduced the viability of CAL-27 human oral cancer cells via gradual release of EA.

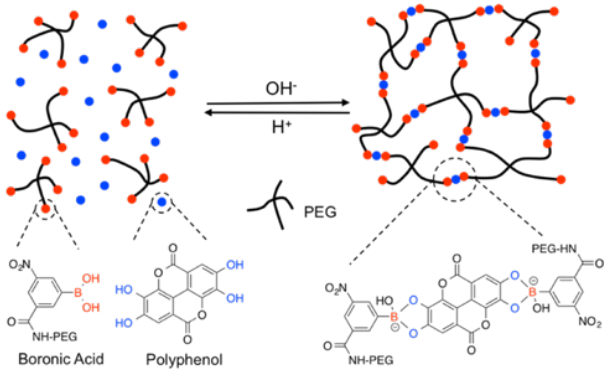

Figure 1. Schematic illustration of pH responsive complexation between boronic acid functionalized PEG and polyphenols resulting in formation of a hydrogel network. The specific boronate ester formed with EA is shown as an example only.

Conclusions: The PEG-BA polymers synthesized here can be utilized in combination with several natural polyphenols as in situ forming injectable hydrogels. The polymer gel is held together by dynamic boronate ester bonds formed spontaneously at physiologic pH. Among the polyphenol linkers investigated in this study, ellagic acid (EA), epigallocatechin gallate (EGCG) and tannic acid (TA) were capable of forming stable hydrogels in physiological condition and displayed potential for *in situ* gelation for oral cancer treatment. In addition to reports on bioactivity of EA, there have been many studies on the possible therapeutic effects of TA and EGCG. Thus, the concept of hydrogel networks exploiting these molecules as dual cross-linker and therapeutic may lead to additional possibilities.

Enzymatically Cross-linked Granular Support Material for Free-form Printing of Soft Materials

Gregory Girardi[1,2], William Hynes[1], Monica Moya[1]

[1]Materials Engineering Division, Lawrence Livermore National Laboratory

[2]Biomedical Engineering Department, University of California, Davis

ABSTRACT

In bioprinting, the creation of a self-healing, non-fissuring, permanent support bath is essential to high-fidelity free-form 3D prints. Currently in the field of bioprinting, support baths are only used during the printing process in order to support the print and once the print is finished the support bath is removed. However **this study focuses on creating a more permanent support bath that remains part of the print post-printing**. This was accomplished by optimizing a popular technique currently used in the field, Free-form Reversible Embedding of Suspended Hydrogels (FRESH). The FRESH technique was optimized by pH adjusting the support bath to increase cell viability in future prints with cell-laden bio-inks as well as the addition of the enzyme transglutaminase (TG), which cross-links gelatin polymers together. With the addition of these methods, the support bath is becoming a viable option for a permanent support material for bioprinting, thus allowing the field to begin to print complex 3D geometries that resemble anatomical structures.

Core-Removal of Hollow Thermoresponsive Sub-Micron Particles for Cell Penetrating Peptide Delivery

Marcus Deloney, Alyssa Panitch.
University of California – Davis Department of Biomedical Engineering.

Introduction: Cell-penetrating peptides (CPPs) have provided a means to facilitate cell uptake of bioactive peptides, proteins and other therapeutics. However, many peptides and proteins are susceptible to proteolytic degradation in the extracellular space, which can limit delivery of the CPP therapeutic to the tissues and cells of interest. We have found that encapsulation of CPPs in thermoresponsive, hydrophilic nanoparticles supports increased uptake of the CPP, and increased efficacy presumably due to CPP-facilitated release from endosomes[1]. However, the NPs were not degradable and have the potential build up in the targeted tissue and cells[1]. The addition of a degradable disulfide crosslinker (BAC) allows the NPs to be broken down and release their full payload. The nanoparticles were composed of poly(n-isopropyl) acrylamide (pNIPAm) copolymerized with 2-acrylamindo-2-methyl-1-propanesulfonic acid (AMPS), acrylic acid (AAc), and crosslinked with N,N'-bis(acryloyl)cystamine (BAC). The addition of a degradable disulfide crosslinker (BAC) allows the NPs to be broken down and release their full payload. To support increased loading and release, particles with low density cores (termed hollow nanoparticles), were synthesized and characterized. A polymer shell was synthesized around non-crosslinked pNIPAm cores above the lower critical solution temperature (LCST) to maintain cores in the polymer rich phase during shell synthesis. The nanoparticles were then dialyzed for 14 days below the LCST, at 4°C, to release the non-crosslinked pNIPAm cores, resulting in hollow nanoparticles. Here we present our current progress in the development of low-density, thermoresponsive, degradable NPs for the increased loading and release of CPP therapeutics.

Materials and Methods: pNIPAM (397.4 mg) cores were synthesized at 70°C for 2 hours in milliQ water under a nitrogen blanket using sodium dodecylsulfate (SDS) (164 µl); polymerization was initiated with potassium persulfate (KPS) (67.4 mg); in some batches fluorescein o-acrylate (FITC) was added (2.5 mg). Following polymerization, the reaction solution was exposed to atmospheric oxygen to terminate free radicals for 45 minutes. The nitrogen blanket was placed over the reaction solution and pNIPAM (794.7 mg), AMPS (87 mg), BAC (48.2 mg), AAc (4.81 µl), and SDS (164 µL) were polymerized around the core using KPS (33.7 mg) to form the shell; in some batches rhodamine B (RHB) was added (4.8 mg). The NPs were purified using tangential flow filtration (TFF) (Spectrum Labs), lyophilized, and divided in half. Half of the NPs were stored serving as the 'solid' sample; the other half was dialyzed below the LCST (4°C) for fourteen days then dialyzed. Dynamic light scattering (DSL) was used for NP diameter. Flow cytometry was used for fluorophore and core removal analysis.

Results and Discussion: FITC-labeled cores diffused out of the RHB-labeled shells when dialyzed below pNIPAM's LCST. Above the LCST, pNIPAM is hydrophobic, and below is hydrophilic, allowing for core-chain removal. Flow cytometry analyzing FITC and RHB excitation and emission show the development of a secondary, FITC negative population post dialysis (blue) in samples that were FITC positive pre-dialysis (red), Figure 1, showing core removal. Additionally, flow cytometry shows no change in RHB concentration in RHB positive NPs pre- and post-dialysis, displaying the shell is unaffected by dialysis/core removal. Figure 2, shows NPs maintain their thermoresponsive behavior and relative size with fluorophore addition.

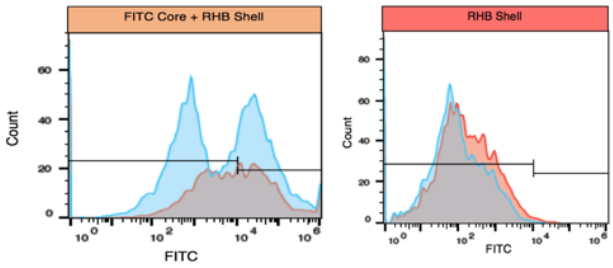

Fig. 1: A) Secondary population of FITC- NPs arise post-dialysis in NPs that are FITC+/RHB+ pre-dialysis; B) FITC-/RHB+ samples remain unaffected by dialysis.

Conclusions: Hollow, degradable, thermoresponsive NPs have been synthesized using solvent free reaction conditions. Dialysis of the cores below their LCST allows for their diffusion out of the disulfide crosslinked shells, as proven by fluorophore addition to the core and/or shell and analyzed by flow cytometry. These hollow, thermoresponsive, degradable NPs will allow for the increase uptake of therapeutics and full payload release at the targeted tissue.

References: McMasters J, Poh S, Lin J, Panitch A. "Delivery of anti-inflammatory peptides from hollow PEGylated poly (NIPAM) nanoparticles reduces inflammation in an ex vivo osteoarthritis model." Journal of Controlled Release. Vol. 258. (2017) 161 – 170.

Injectable Composite Hydrogels for Bone Repair in a Sheep Bone Defect Model

Marissa Gionet-Gonzales[1], Ganesh C. Ingavle[1], Charlotte Vorwald[1], Laurie K. Bohannon[2], Kaitlin Clark[2], Larry D. Galuppo[2], J. Kent Leach[1,3]*

[1]Department of Biomedical Engineering, University of California, Davis, Davis, CA 95616
[2]Department of Surgical & Radiological Sciences, UC Davis School of Veterinary Medicine, Davis, CA 95616
[3]Department of Orthopaedic Surgery, School of Medicine, UC Davis Health, Sacramento, CA 95817

Statement of Purpose: Effective cell-based therapies for bone healing require the delivery of cells using instructive biomaterials that localize cells at the target site and provide instructional cues. Hydrogels are widely used in such applications, as they are chemically and physically tailorable, but they often lack the desired osteoconductivity of other common materials. To address this shortcoming, we entrapped mesenchymal stem cells (MSCs) in a novel composite hydrogel with enhanced osteoconductivity to promote bone regeneration in an ovine iliac crest bone defect. The composite hydrogel was composed of alginate, chosen for its tailorability, and hyaluronate, selected for its engagement of the CD44 cell receptor present on MSCs. Arginine-Glycine-Aspartic Acid (RGD) was conjugated to the backbone of both polymers to facilitate cell adhesion. Hydrogel osteoconductivity was increased by incorporating biomineralized polymeric microspheres into the network. We hypothesized that the transplantation of autologous ovine MSCs within this composite hydrogel containing mineralized polymeric microspheres would enhance hydrogel osteoconductivity, increase osteogenic potential, and promote bone healing in an ovine bone defect model.

Methods: Bone marrow was collected from 12 adult female Swiss Alpine sheep. Red blood cells and plasma were then removed from the aspirate, and the remaining cells were expanded and used for implantation. Sodium alginate was irradiated at 5 Mrad for faster degradation and covalently modified with G_4RGDSP using standard carbodiimide chemistry. Similarly, G_4RGDSP was covalently coupled to sodium hyaluronate using similar protocols. Poly(lactide-*co*-glycolide) (PLG) microspheres were formed using a double-emulsion process and underwent biomineralization by incubation in modified simulated body fluid. The gels were produced by mixing a 2% RGD-alginate and 1% RGD-hyaluronate at a 1:9 ratio with microspheres at a 3 mg/mL concentration. Control hydrogels were formed of RGD-alginate or RGD-alginate/hyaluronate (lacking RGD). Ovine MSCs were entrapped at 10 million cells/mL, and the gel was crosslinked *via* a supersaturated solution of $CaSO_4$. The hydrogels were characterized through SEM, NMR and mechanical testing. The osteogenic response of MSCs within the gel during *in vitro* culture was quantified by ALP expression and calcium deposition. Composite hydrogels were then injected into bilateral critical-sized iliac crest bone defects in adult female Swiss Alpine sheep. Repair of the bone defect at 12 weeks was evaluated through radiography, microCT and histology.

Results: NMR data confirmed that RGD was conjugated to both the hyaluronate and alginate. Alginate and alginate hyaluronate composite hydrogels exhibited similar swelling ratio and gross morphology. However, the compressive modulus and pore size decreased when hyaluronate was added. MSCs cultured in RGD-alginate/RGD-hyaluronate for 3 weeks had increased ALP activity and calcium accumulation compared to MSCs in RGD-alginate or RGD-alginate/hyaluronate. Therefore, RGD-alginate/RGD-hyaluronate gels were used for implantation. At 12 weeks, microCT revealed that bone defects treated with MSC-containing composite hydrogels had higher bone volume fraction and bone mineral density compared to sham and acellular groups (**Figure 1**). Histology indicated this group exhibited the highest vessel density. H&E, Masson's trichrome and Goldner's trichrome further confirmed more bone growth and collagen deposition within defects treated with MSC-containing gels.

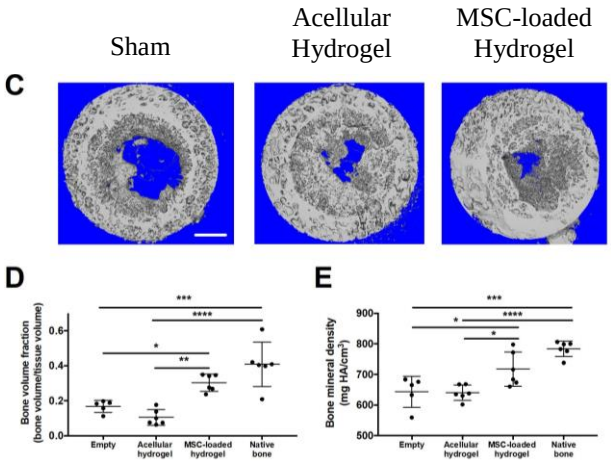

Figure 1. A) Representative microCT images at 12 weeks. Scale bar = 3 mm. (B) Bone volume fraction within the tissue defects. (C) Bone mineral density within the tissue defects. N=5-6; **p*<0.05, ***p*<0.01, ****p*<0.001, *****p*<0.0001

Conclusions: We have successfully developed and characterized a composite hydrogel formed of RGD-modified alginate and hyaluronate that contained apatite-coated polymeric microspheres. This material increased the osteogenic response of ovine MSCs *in vitro* while serving as an effective cell carrier for MSCs to promote bone regeneration and neovascularization in a sheep iliac crest defect. These data also reveal that RGD-hyaluronate, a material that engages both CD44 and RGD receptors, can enhance osteogenic differentiation to a greater degree compared to gels that engage each receptor alone. In light of these findings and its contribution to connective tissue homeostasis, the use of hyaluronate in instructive hydrogels merits consideration for use in other platforms designed to promote bone healing.

Trojan Horse nanotheranostics with dual transformability and multifunctionality for highly effective cancer treatment

Xiangdong Xue, Yee Huang, Ruonan Bo, Bei Jia, Hao Wu, Ye Yuan, Zhongling Wang, Zhao Ma, Di Jing, Xiaobao Xu, Weimin Yu, Tzu-yin Lin, Yuanpei Li, *

Department of Biochemistry and Molecular Medicine, UC Davis Comprehensive Cancer Center, University of California Davis, Sacramento, CA 95817, USA;

*Corresponding author (Y.L: lypli@ucdavis.edu)

Nanotheranostics with integrated diagnostic and therapeutic functions show exciting potentials towards precision nanomedicine. However, targeted delivery of nanotheranostics is hindered by several biological barriers. The barriers mainly prevent the therapeutics from reaching the targeting tumor cells, include i) undesirable circulation time due to blood shear stress, opsonization and renal clearance; ii) limited tumor tissue penetrations due to the high interstitial fluid pressure and dense extracellular matrix in tumor microenvironment (TME); iii) ineffective cell internalization and iv) inefficient intracellular drug release, etc. Generally, these barriers cannot be circumvented simultaneously, due to the existence of some contradicts. For instance, the ultra-stable nanoparticles can stand the blood shear stress but may not release the drug effectively; larger nanoparticles prevent the renal clearance but blunts the penetration; negatively charge avoids opsonization but plummets the cell uptake. Therefore, the balance of those contradicts is very important.

Here, we developed a dual size/charge- transformable, Trojan-Horse nanoparticle for delivery of ultra-small, 100% active pharmaceutical ingredients (API) nanotheranostics with integrated dual-modal imaging and trimodal therapeutic functions. The Trojan-Horse nanoparticles could smartly balance the biological barriers during the drug delivery. In the blood vessel, the nanoparticles exhibit ideal size and surface charge for drug transportation; When they encounter the tumor micro-environment, the Trojan-Horse nanoparticles responsively transform to 100% API nanotheranostics with ultra-small size and higher surface charge, which dramatically facilitate the tumor penetration and cell internalization. The Trojan-Horse nanoparticle also showed excellent imaging capabilities, which visualized the biodistribution of the nanotheranostics by near-infrared fluorescence imaging (NIRFI), tumor accumulation and therapeutic effect of the nanotheranostics by magnetic resonance imaging (MRI). Moreover, the synergistic photothermal-, photodynamic- and chemo-therapies achieve a 100% complete cure rate on both subcutaneous and orthotopic oral cancer models, due to the highly effective drug delivery ability of the Trojan-Horse design.

This transformable, Trojan-Horse liked nanoplatform with integrated powerful delivery efficiency and versatile theranostic functions are expected to open a broad range of possibilities to improve cancer management. It will also inspire other scientists to develop next generation smart nanomaterials for a variety of biomedical application.

Nanoporous Gold as a Multifunctional Neural Electrode Coating

Christopher A. R. Chapman[1], Özge Polat[2], Zidong Li[1], Pallavi Daggumati[3], Noah Goshi[1], Jovana Veselinovic[2], Hao Chen[4], Marianna Stamou[4], Ling Wang[3], Alex Hampe[1], Juergen Diener[5], Monika Biener[5], Manyalibo Matthews[5], Pamela Lein[4], Erkin Şeker[3]

Abstract: Neural electrodes constitute an important tool for monitoring and modulating the electrophysiological activity of the nervous system. One obstacle in long-term reliability of neural recording electrodes has been the undesired aggregation of glial cells on the surface of the electrode and subsequent death and/or detachment of neurons from the electrode surface. Among different strategies to enhance the neuron-electrode interface, multifunctional electrode coatings have shown promise. Nanoporous gold (np-Au), produced by a nano-scale self-assembly process, is a relatively new material and has mostly attracted attention for catalyst applications due to its high effective surface area, electrical conductivity, and ease of surface functionalization. Surprisingly, the biomedical potential of this material has remained largely untapped. Here, we will discuss our research group's efforts that reveals nano-/micro-scale properties of np-Au and the application of micropatterning techniques for fabricating high-fidelity multiple electrode arrays for neural electrophysiology studies. Specifically, we will illustrate how tunable properties of np-Au (e.g., surface topography and chemistry) are utilized to enhance the recording fidelity in organotypic brain slice and primary cortical cell cultures. To that end, we will focus on (i) np-Au's in situ drug delivery performance (dictated by molecule-surface interactions and mass transport in nanofluidic pore network); (ii) np-Au's performance in selectively reducing astrogliosis while maintaining high neuronal coverage (driven largely by topographical cues); and (iii) np-Au's biofouling-resilience in preventing the permeation of large biomolecules while allowing ionic transport to sustain electrochemical activity and electrophysiological recordings. These features taken together identifies np-Au as a promising material for multifunctional neural electrode coatings.

Cell Type-Specific Surface Attachment: Aggregation of glial cells on the surface of neural electrodes, and the subsequent death and/or detachment of neurons from the electrode surface is one of the leading causes for the loss of functionality of neural implants. One promising strategy to enhance the neuron-electrode coupling, is to use topographical cues to produce cell type-specific differences in attachment to the underlying electrode. We examined the difference in astrocyte versus neuron surface coverage of primary rat cortical neuron-glia co-cultures grown on planar gold (pl-Au) and np-Au. Quantitative fluorescence microscopy revealed that while there was no statistical difference between neuronal coverage ($p > 0.9$) on the two coatings, astrocyte coverage was drastically reduced on np-Au as compared to pl-Au ($^*p < 0.001$).

In Situ Drug Delivery: Another benefit of np-Au as an electrode material is the ability to use the np-Au as a drug delivery material. We demonstrated that np-Au thin films retained a significant amount of fluorescein (used as a small molecule drug surrogate), and the release rate could be tuned by changing film morphology. We verified this capability by measuring astrocyte proliferation on np-Au spots loaded with the anti-mitotic drug Ara-C, and showed a decrease in astrocyte cell coverage in a dose-dependent manner to Ara-C release from loaded np-Au samples. Additionally, by using alumina-coated np-Au electrodes, we were able to electrically control the release of fluorescein to produce arbitrary concentration waveforms.

Departments of [1]Biomedical Engineering, [2]Chemical Engineering, [3]Electrical & Computer Engineering, [4]Molecular Biosciences, University of California Davis, CA 95616; [5]Lawrence Livermore National Laboratory, Livermore, CA 94550

The Importance of Classical Elastica Theory in Microtubules Buckling

Fereshteh Memarian[1], Daniel Beller[1], Linda Hirst[1]
1 Physics Department of University of California, Merced

Abstract

The classical Bernoulli-Euler Elastica theory is for the curve of an elastic rod. Daniel Bernoulli found the energy function of an elastic rod and Leonhard Euler solved it for certain situations by his own elliptic integral theory.

When the filamentous particles buckle to each other the configuration is similar to the Elastica curve. In a homogenous and stable system, filaments-bundle prevents violent jumps, non-uniqueness and hysteresis. Elastica theory assists us in understanding the deformation and bending of filamentous particles, for instance, deformation of microtubules (MTs), which is still unexplored in some aspects.

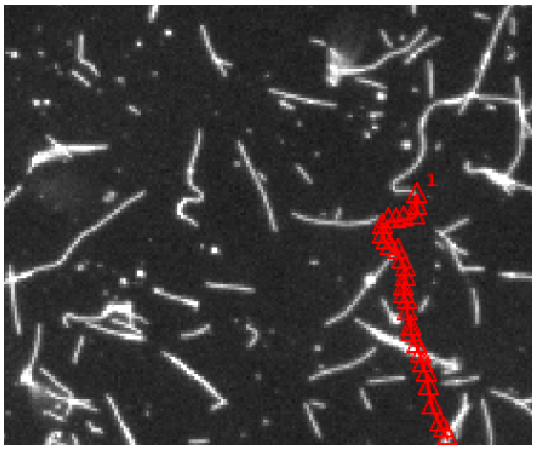

Fig1: Dynamical shapes of microtubules and tracking tail of an individual microtubule (see Red triangles) on a glass. [Hirst Lab]

In this work, the mathematical history, bending energy of an individual microtubule and its Euler-Lagrange equation will be discussed. Moreover, the mechanical behavior of polymerizing and depolymerizing of the MTs is not well known and I will focus on it by using the classical Elastica theory. In future work, the relation between bending moment and curvature and the exact solution for a certain situation will be investigated.

Reference:

- Hermes Gadelha, The filament-bundle Elastica, IMA Journal of Applied Mathematics, 83(4):634-654, 2018
- Shigeki Matsutani, Euler's Elastica and beyond, itshape{Journal of Geometry and Symmetry in Physics, 17:45-86, 2010
- Alberts, Bruce; Johnson, Alexander; Lewis, Julian; Raff, Martin; Roberts, Keith; Walter, Peter., Molecular biology of the cell, 4th edition, New York, Garland Science, 2002, ISBN-10: 0-8153-3218-1
- Raph Levien, The elastica: a mathematical history, EECS Department University of California, Berkeley, Technical Report No. UCB/EECS-2008-103, 2008
- Ivaïlo M. Mladenov, Mariana Hadzhilazova, The many faces of Elastica, Springer International Publishing, Vol 3, 2017, ISBN: 978-3-319-61242-3
- Kabir, A. M. R. et al., Buckling of Microtubules on a 2D Elastic Medium, Sci.Rep.5, 17222, 2015

Development of an Exosome-mimic for Vascular Regeneration in Ischemic Wound Sites

Lalithasri Ramasubramanian[1], Aijun Wang[1]
[1]University of California, Davis

PURPOSE

Exosomes are nanovesicles (50-150 nm) secreted through the invagination of plasma membranes of cells and released to mediate critical cell functions, including cell proliferation, angiogenesis, and immunomodulation. Specifically, exosomes derived from endothelial progenitor cells (EPC) increase the recruitment and proliferation of EPCs and endothelial cells (ECs) to facilitate angiogenesis via release of microRNAs, namely miR-126. However, therapeutic translation of exosomes has been greatly hindered by the inherent disadvantages in exosome isolation, purification, and standardization. To overcome the disadvantages of native exosomes, we hypothesize that a biomimetic synthetic exosome can be synthesized by engineering a miR-126-loaded poly(lactic-co-glycolic acid) (PLGA) nanoparticle with a LXW7-functionalized EPC-membrane shell in order to recapitulate the pro-angiogenic, targeting, and cell recruiting properties of native EPC-derived exosomes.

METHODS

PLGA core synthesis. A nanoprecipitation method was used to synthesize PLGA cores. PLGA and DiI, a lipophilic dye used as a proof-of-concept molecule in place of miR-126, was emulsified in an organic phase composed of acetone. The emulsion was added slowly dropwise to an excess of aqueous phase (deionized water) under constant stirring. The solution was stirred under open air to allow for the excess acetone to evaporate. The PLGA cores were then collected and purified using centrifugal filtration and subsequently resuspended in water.

Plasma membrane (PM) coating. Placenta-derived mesenchymal stromal cell (PMSC) plasma membranes were isolated to establish proof-of-concept. PMSCs were lysed with a combination of hypotonic lysis buffer and mechanical disturbance to obtain a lysate from which the PM fraction was isolated through serial centrifugation. The PM fraction and PLGA cores were coextruded through 200 nm polycarbonate membranes to obtain cell-membrane coated nanoparticles (CMNPs).

RESULTS

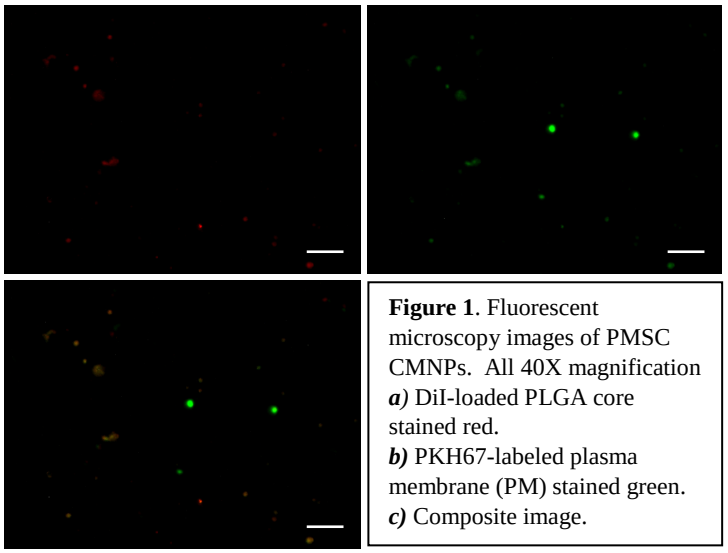

Figure 1. Fluorescent microscopy images of PMSC CMNPs. All 40X magnification
a) DiI-loaded PLGA core stained red.
b) PKH67-labeled plasma membrane (PM) stained green.
c) Composite image.

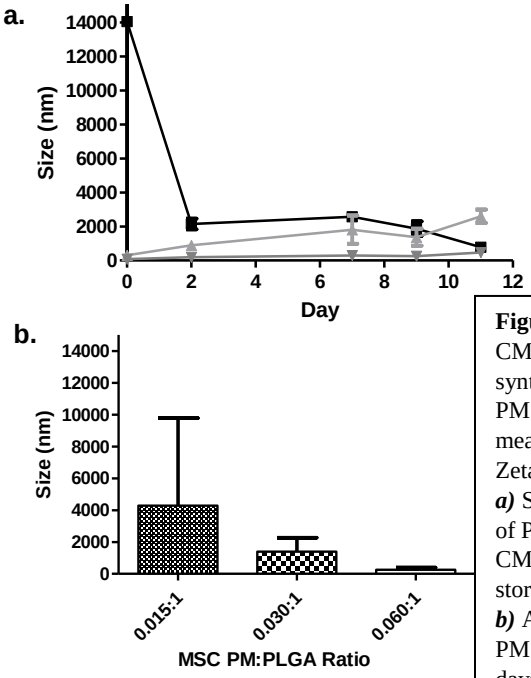

Figure 2. PMSC-coated CMNPs were synthesized at different PM:PLGA ratios and measured by Malvern Zetasizer.
a) Size of different ratios of PM:PLGA PMSC CMNPS over 11 days stored in 1X PBS at 4°C.
b) Average size of PMSC CMNPs over 11 days. All measurements were taken in triplicate.

CONCLUSION

- Plasma membrane can be successfully coated on PLGA core nanoparticles.
- 0.060:1 PMSC PM:PLGA ratio yields the most stable CMNPs of size ~200 nm.
- Molecules can be loaded within PLGA core using DiI as a proof-of-concept cargo.

Future work

- Further optimization to decrease size to ~100 nm and to improve stability over longer time.
- Loading miR-126 and LXW7 functionalization.
- Examine angiogenic potential with *in vitro* cell proliferation, scratch, and tube formation assays.
- *In vivo* assessment using murine hindlimb ischemic model.

Fabrication of Hydroxyapatite –Poly(lactide-co-glycolide) Composite Scaffolds with Reproducible Pore Geometry for Improved Cellular Infiltration and Alignment

Takeyah Campbell, B.S.[a], Jonathan Chen, B.S.[a], Jenna Harvestine, Ph.D.[a], Kent Leach, Ph.D.[a, b]
[a]Department of Biomedical Engineering, University of California, Davis, Davis, CA 95616
[b]Department of Orthopaedic Surgery, UC Davis Health, Sacramento, CA 95817

Statement of Purpose: Bone tissue engineering often employs cell instructive biomaterials to enhance the osteogenic potential and proliferation of cells *via* mechanical cues. Composite scaffolds formed of hydroxyapatite-poly(lactide-co-glycolide (HA-PLG) effectively support osteogenic differentiation, proliferation, and trophic factor secretion by associated mesenchymal stem cells during *in vitro* culture. Biophysical properties of scaffolds including pore interconnectivity and diameter influence cell expansion and differentiation. However, most widely used scaffold manufacturing methods lack necessary control of pore geometry, thereby limiting uniformity, reproducibility, or the preferred osteogenic-inducing formulations. To address these challenges, we designed a solvent extraction/laser cut method to manufacture HA-PLG scaffolds with reproducible geometries and preferred composition (HA-PLG mass ratio) to facilitate osteogenic differentiation.

Methods: Molds were fabricated from a Delrin case and silicone resin, and Teflon-coated stainless steel wires were horizontally positioned in the mold. Scaffolds with horizontal pores were formed by adding a mixture of HA and PLG at a 2.5:1 mass ratio previously dissolved in acetone. Vertical pores were added and the scaffold was shaped *via* a CAD model using a Kern Micro24 150W CO_2 laser cutter. Mouse pre-osteoblasts (MC3T3-E1) were seeded and cultured on sterilized gas foamed or laser cut scaffolds, and we measured cell proliferation and scaffold cytotoxicity.

Results: Laser cut scaffolds had pore diameters of 417±21 µm, while gas foamed scaffolds had pores of 250-425 µm diameter. After 2 days in culture, preliminary data revealed there was a significant increase in DNA content for laser cut scaffolds compared to their gas-foamed counterparts (**Fig. 1A**). We did not detect significant differences in metabolic activity in each group (**Fig. 1B**), indicating that manufacturing processes did not impair cell adhesion or metabolic activity. Cell distribution appeared uniform throughout laser cut scaffolds *via* DAPI and H&E staining (**Fig. 1C**).

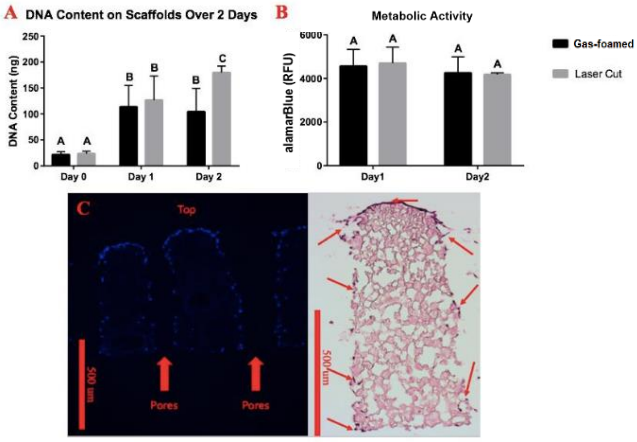

Figure 1: Cytotoxicity testing on solvent extracted – laser cut scaffolds. A. DNA content of gas-foamed and laser cut scaffolds. **B.** alamarBlue fluorescence signal of gas-foamed and laser cut scaffolds over two days. Data are mean ± SD, n=6. Bars with different letters represent data that are significantly different. **C.** DAPI (left) and H&E (right) staining of laser cut scaffold.

Conclusions: We demonstrated that the pore geometry and suitable osteogenic formulations in macroporous HA-PLG composite scaffolds can be readily controlled and reproduced *via* the solvent extraction/ laser cutting method. These scaffolds enable increased cell expansion compared to gas-foamed scaffolds with no apparent cytotoxicity. In future experiments, we will investigate the osteoconductive potential of these scaffolds.

Selectin-targeting molecule acts as an antagonist to neutrophil adhesion and fibrosis

Tima Dehghani[1], Phung Thai,[2] Hark Sodhi[1], Alyssa Panitch[1]
[1] Department of Biomedical Engineering, University of California Davis, Davis, CA 95616
[2]Department of Pharmacology, University of California Davis, Davis, CA 95616

Purpose

Maintaining healthy blood vessel phenotype is a complex process that requires in part the coordination of endothelial cells (EC), circulating immune cells, and secreted cytokines and chemokines. During an inflammatory insult, many if not all of these components are disturbed. On the endothelial side, this manifests as EC dysfunction, a disorder characterized by the loss of the glycocalyx, a thin glycosaminoglycan-rich layer on the EC surface, which provides a protective interface that regulates immune cell adhesion. We have recently discovered a selectin targeting anti-adhesive coating (termed EC-SEALd) consisting of a dermatan sulfate (DS) backbone and multiple selectin-binding peptides that profoundly diminished the ability of neutrophils to migrate through inflamed endothelium into the peripheral tissue. Data indicate increased infiltration of neutrophils occurs in various tissues, such as heart and lung, as a result of endothelial insult and inflammation. Therefore, a molecule that provides a stable, stealthy interface with the capacity to down-regulate neutrophil capture and transendothelial migration could tip the balance in maintaining homeostasis in inflammation-induced disease.

Methods

Neutrophil binding to E-selectin coated microspheres: Recombinant human E-selectin is conjugated to carboxyl microspheres. Microspheres are then treated with Hank's Balanced Salt Solution (HBSS), DS, peptide alone, or EC-SEALd for 1 hour. Microspheres are spun down and resuspended in fluorescently labeled isolated human neutrophils for 30 minutes. Samples are fixed in 4% paraformaldehyde and run on an Attune NxT flow cytometer.

Ischemia Reperfusion: 10-12 week old C57BL/6J mice undergo 45 minutes of ischemia at the left anterior descending artery. Ischemia is verified by ST segment elevation on an electrocardiogram. Animals are injected with 30 µM EC-SEALd or saline after reperfusion and suture, and again at 24 hours. Echo is performed at baseline and 2 weeks after ischemia/ reperfusion to evaluate cardiac function. At 2 weeks, mice are euthanized, and hearts harvested for histology. Degree of fibrosis quantified by Picrosirius Red and Masson's Trichrome staining.

Results

Neutrophil binding to E-selectin coated microspheres: EC-SEALd achieves comparable neutrophil antagonism as the parent molecule, EC-SEAL, with fewer peptides.

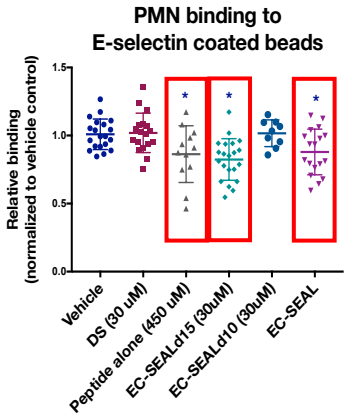

Ischemia Reperfusion: Treatment with EC-SEALd reduces collagen deposition and improved fractional shortening in the left ventricle as compared to saline after 45 minutes of ischemia, as well as increased fractional shortening.

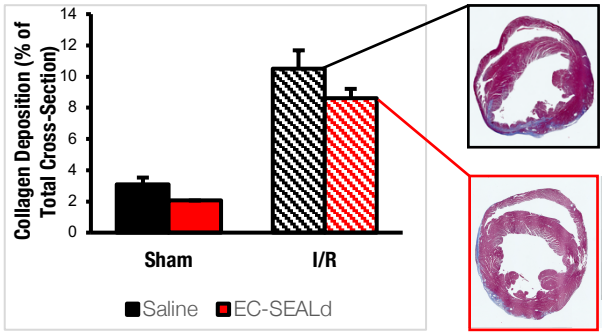

Conclusions

Our results suggest EC-SEALd is a promising replacement for EC-SEAL, and has potential as an anti-fibrotic molecule.

Thaw-Induced Gelation for the Encapsulation of Cryopreserved Cells in Alginate Capsules

Dustin Hadley and Eduardo Silva
Department of Biomedical Engineering, University of California, Davis

Purpose: Alginate is a naturally occurring biocompatible polysaccharide that offers rapid ionic hydrogel gelation with divalent cations. Moreover, cells do not adhere to alginate, making it an appealing biomaterial to promote spheroid formation. Despite the growing interest in spheroids for tissue engineering and drug discovery, their application with cryopreservation strategies has been understudied. Previously, our lab has developed the method of thaw-induced gelation (TIG) for alginate to generate distinct hydrogel structures for controlling cargo release. We hypothesize that TIG can encapsulate cryopreserved human embryonic kidney cells (HEK-293T) and encourage spheroid formation. The method shows promise in generating spheroids from cryopreserved cells.

Methods: The method for encapsulating cells by TIG of utilizes a cell freezing solution containing an alginate crosslinker and alginate thawing solution. HEK-293T cells were used as a cell-line known to form aggregates. This freezing solution is then frozen following standard slow cooling cryopreservation protocols in molds. TIG was initiated by dropping frozen samples into an alginate solution. We observed encapsulated cells over 5 days to investigate aggregation. Initial viability of cells without gelation and metabolic activity were calculated via a trypan blue exclusion assay and an MTT assay, respectively.

Results: The formation of alginate hydrogel capsules via TIG was dependent on both the crosslinker and polymer concentrations. Increasing crosslinker or polymer concentrations led to an increase in hydrogel shell thickness and a decrease in mesh size. Although the addition of crosslinker had no statistically significant ($p>0.05$) effect on initial viability of the cells, remaining above 85%, as the crosslinker concentration increased above isotonic salinities there was a significant decrease in metabolic activity compared to an unmodified freezing solution. However, these capsules were able to support the formation of spheroids by day 3 (Fig. 1A), and they were growing between day 3 and day 5 (Fig. 1B).

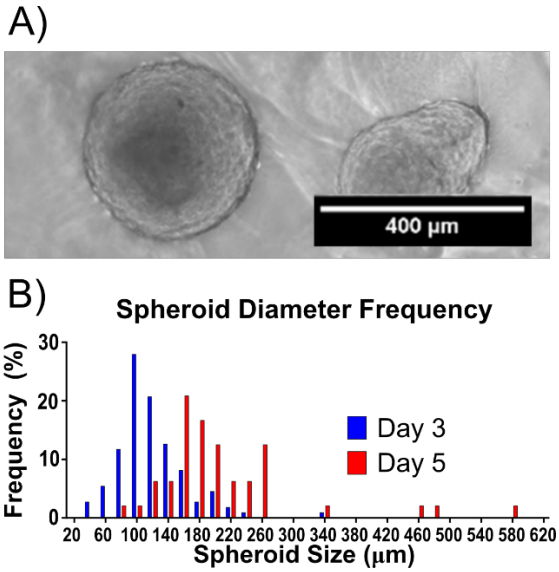

Figure 1. Spheroid formation and expansion within TIG alginate hydrogels.

Conclusion: We developed a gelation process that encapsulates cryopreserved cells in a hydrogel while thawing. To our knowledge, this is the first instance of using thaw-induced gelation of a biomaterial to encapsulate cells. Moreover, this encapsulation promotes spheroid formation, which is promising for the development of patient-derived cell aggregates in tissue engineering and organoids for drug discovery. Future studies will be applying this method for revascularization strategies.

Characterizing the encapsulation and release of lentivectors and adeno-associated vectors from degradable alginate hydrogels

Shahin Shams, Justin Madrigal, Roberta Stilhano, and Eduardo Silva
Department of Biomedical Engineering, University of California, Davis

Purpose: Gene therapies have been licensed for use by the FDA since 2017. Approved gene therapies utilize lentivectors (LV) or adeno-associated vectors (AAV), and many future applications of these vectors will benefit from methods of localizing and controlling their delivery for therapeutic administration. Degradable alginate hydrogels have shown promise as delivery vehicles for vector payloads. Utilizing two different degradable alginate hydrogel formulations, we compare the ability of alginate hydrogels to efficiently encapsulate and deliver LV (hydrodynamic radius 166nm) and AAV (hydrodynamic radius 29nm). We hypothesize that physical properties of the viral vector and delivery vehicle impact the release of viral particles.

Methods: 2% alginate hydrogels of slow degrading formulation (75:25 ratio 1% oxidized LF10/60 and 1% oxidized LF20/40) or fast degrading formulation (80:20 ratio of 5% oxidized LF20/40 and non-oxidized LF10/60) crosslinked with calcium carbonate and gluconic acid delta-lactone were used to encapsulate multiplicity of infection (MOI) = 10 of LV or AAV. Physical properties of both hydrogel formulations initially and over time were determined by rheometry. Viral loaded disks were placed in media, and this media was collected and replaced every 24 hours for 5 days to quantify release by either real time PCR (AAV) or ELISA (LV).

Results: The two degradable alginate hydrogel formulations differed significantly in their initial mesh size (Fig. 1A). Release of larger LV particles from alginate hydrogels was dependent on hydrogel degradation (Fig.1B), while release of smaller AAV relied on a diffusive mechanism and was independent of the formulation used (Fig. 1C).

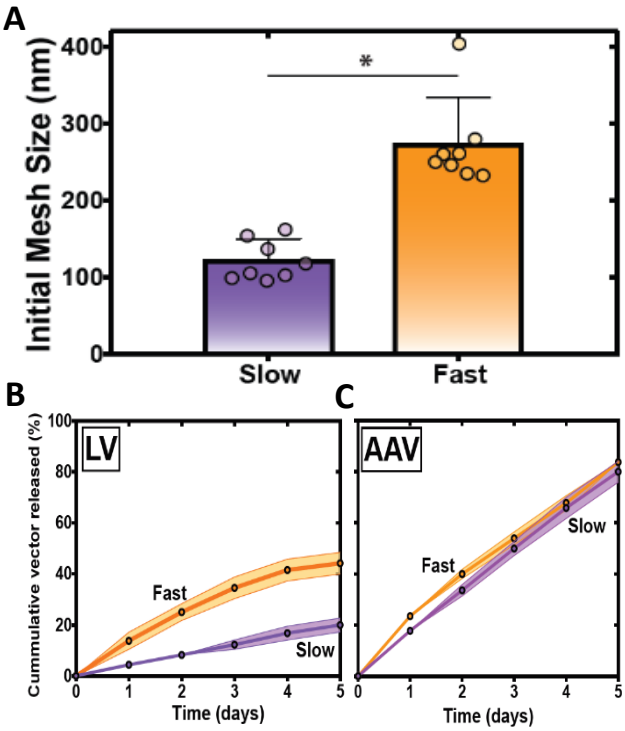

Figure 1: Initial mesh size of slow and fast degrading formulation hydrogels (A). LV (B) and AAV release (C) over time.

Conclusion: We have shown that alginate hydrogels can successfully encapsulate LV and AAV, and that vector release was dependent on different mechanisms. To our knowledge this is the first direct comparison of LV and AAV release and the first ever study of AAV release from degradable alginate hydrogels. Future studies will focus on tuning the physical properties of alginate hydrogels for the controlled release of AAV.

Sol-gel derived mesoporous silica is routinely used to immobilize soluble proteins for development of novel biomaterials with applications in high throughput devices, biosensing, chromatography and so on. However, membrane proteins such as GPCRs, constituting 40% of drug targets have not been successfully entrapped in silica for high throughput drug discovery. In this work, Bacteriorhodopsin which is a transmembrane protein from *Halobacterium Salinarum,* was used as a model protein for GPCRs and immobilized in sol-gel derived silica in its native purple membrane form. The amount of alcohol evolved in sol-gel synthesis was minimized via rotary evaporation to avoid protein denaturation. Absorbance spectrum of the protein has a characteristic peak at 560 nm due to its bound chromophore which is present after encapsulation depicting retention of the protein's tertiary structure. Intrinsic tryptophan fluorescence was used to investigate the microenvironment of the encapsulated protein. A decrease in emission intensity with temperature was observed for the protein in solution and in the gel. It was determined that the effect of local pH around the protein has a significant effect on the observed trends. The protein was much more stable at higher temperatures when the pH was closer to neutral in silica gel pore environment. Fluorescence anisotropy with change in temperature also showed consistent trends with more unfolding of protein at higher temperatures. Solvent accessibility determined using acrylamide quenching of tryptophan residues indicated similar environment for the tryptophan residues before and after entrapment. CD spectroscopy was used to investigate the changes in secondary structure of the protein before and after entrapment in silica which shows the alpha helical structure of the protein. This work provides the groundwork for development of biocompatible mesoporous silica for membrane protein encapsulation. In future, Bacteriorhodopsin will be expressed in lipid bilayer nanodiscs and immobilized in silica monoliths where this work would be used for comparative studies to understand the effect of membrane structure on protein stability.

Coupled flow and osmotic stress driven directed movement of vesicles

Abstract

How cells move in response to concentration gradients has been a subject of intense research. Understanding response of membrane to concentration gradients will shed light on the origins of membrane bound compartments and active movement. Here we use artificial vesicles made from DMPC lipid to simulate membrane bound cellular movement in response to osmotic concentration gradients. The strategic choice of lipid here allows tuning the permeability and bio-mechanical parameters such as tension and rigidity by changing the temperature. Our preliminary observations indicate a membrane bio-mechanics based predictive coupling between flow induced tension and osmotic stress induced morphological transitions. At the phase transition temperature of the lipid, flow and osmotic stress together generate directed movement while displaying pearling of the vesicles into smaller compartments. Current work is focused towards decoupling the flow and osmotic stress to observe the role of deliberate steady state osmotic gradients in the absence of flow on morphological response of the vesicle. Since cells contain actin network that contribute to the overall mechanical response of the cell to osmotic gradients, vesicles with various configurations mimicking actin framework is being constructed. These observations can give insights into the origins of compartments in cells in primitive earth and shows promising therapeutic drug-delivery applications.

Purpose:

To understand the role of flow coupled as well as decoupled osmotic stress in self-propelled motion and compartmentalization using simplified artificial cell mimics called vesicles.

Methods:

Giant vesicles were generated using Electroformation method. Vesicles were visualized using florescence microscopy setup. Microfluidic channels were designed to generate constant osmotic gradients.

Results:

Vesicles respond to osmotic differences by undergoing dramatic morphological changes. Addition of high concentration (300mM) (added from one end) glucose on the outside creates hypertonic stress as well as flow which squeezes water from the vesicle. Below phase transition temperature, since thermal undulations are less, the response of the vesicle is dominated by flow causing vesicles to move. At higher temperatures, the response of the vesicle is dominated by the osmotic stress which causes vesicles to display vivid shape dynamics. At phase transition temperature however, both flow and osmotic stress play a significant role causing the vesicle to move while displaying vivid morphological deformations. More interestingly our observations show that the vesicle almost exclusively display pearling while moving away from the point of addition of hypertonic solute.

Next, we demonstrated generation of osmotic gradients using microfluidic channels. However, the gradients are short lived and require further testing. Lastly, we successfully developed vesicles containing actin filaments for the second phase of the project.

Conclusion:

We demonstrated that semipermeable membrane vesicles can respond to osmotic stress and set in directed motion whist displaying vivid morphologies. In future we will work towards generation of perpetual gradients stable for days. These design principles will be exploited to generate non-equilibrium systems to understand the role of gradient forces in the origins of life, development of soft robotic systems for ultra-sensitive active drug delivery vehicles using Osmo-responsive drug loaded lipidic vesicles.

Introduction: Rheumatoid arthritis (RA) is a chronic, disabling autoimmune condition afflicting about 0.3 – 1% of the world's adult population[1]. One potential avenue for treatment of RA is the development of RA-specific tolerogenic dendritic cells (tDCs). Tolerogenic DCs are an attractive solution for treatment of RA in that they target the immune cascade responsible for RA, rather than addressing the symptoms as with most convention therapies. Previously, it has been demonstrated that exogenously-treated tDCs can limit autoimmunity in a RA murine model[2]. However, *ex-vivo* stability and manufacturing cost inhibit the widespread use of exogenously-treated tDCs in autoimmune treatments.

In an effort to circumvent drawbacks with exogenously-derived tDC therapy, an "anti-vaccine" (avacc) delivering tolerogenic factors via poly (lactic-co-glycolic acid) (PLGA) microparticles (MPs) that passively target DCs has been explored as a potential system for autoimmune disease treatment[3]. **Our *working hypothesis* is that this avacc will modulate DC phenotype *in vivo*, thus affecting antigen presentation and co-stimulation, ultimately suppressing autoimmunity in a collagen-induced arthritis (CIA) murine model.**

Methods: 30 DBA/1J mice were injected intradermally in the tail with an emulsion of Complete Freund's Adjuvant (CFA) and bovine collagen II. Affected mice were continually monitored for arthritic severity using an established clinical scoring[2]. Phagocytosable PLGA MPs (1 μm) loaded with collagen II or Vitamin D3 [1α, 25-dihydroxycholecalciferol] (denatured) were synthesized for intracellular uptake by DCs[3]. Additionally, unphagocytosable MPs (30 μm) were fabricated to deliver the immunomodulatory factors TGF-β1 or GM-CSF to both recruit DCs to the injection bolus and suppress pro-inflammatory collagen reactions downstream[3]. Treatment groups included Naïve, CIA+ (positive control) and MP avacc (Vit D3 MPs + Col II MPs + *TGF-β1 MPs* + *GM-CSF MPs)*. Once mice had become arthritic (clinical score of 5), MP injections were given on day 1, 3, and 7, followed by biweekly boosters. Terminal [day 56 (t56)] and mid-study [day 28 (t28)] assessments to establish RA progression included [18-F]DG PET imaging, histology of paws, cytokine secretion via RT-PCR and various cellular phenotypic analyses.

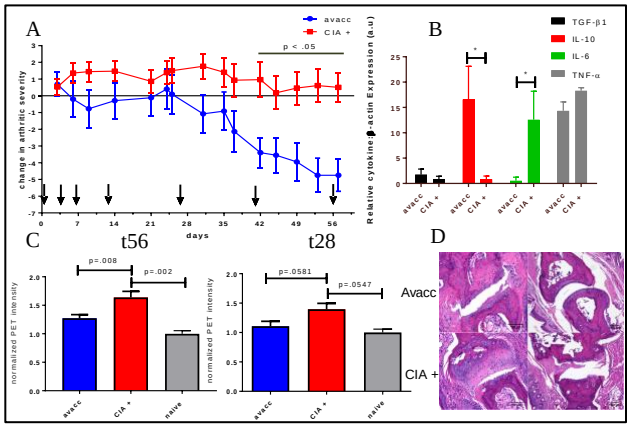

Figure 1. (a) MP treated mice show decrease in clinical scores (arthritic severity) over time, arrows represent MP injection (b) RT-PCR analysis shows decreased levels of mRNA for IL-6 and increased levels of IL-10 for avacc treated mice (* represents a statistically significant difference between the two groups; p<.05). (c) PET analysis shows significant decrease in PET intensity for the avacc group at t56, but not at t28 (d) Histopathological analysis of avacc treated groups showed decreased cellular infiltration and cartilage degradation.

Results: Both phagocytosable and unphagocytosable PLGA MPs were successfully synthesized and physicochemically characterized (**not shown**). Particles were co-cultured with bone marrow derived DCs and macrophages *in vitro*; treated cells showed suppressed allogeneic T cell proliferation in a mixed lymphocyte reaction (**not shown).** CIA clinical scores of the MP treated groups decreased as the study progressed, becoming significantly lower at 42 days post-initial injection (t42) (**Figure 1a).** RT-PCR analysis at t56 in the paws of treated mice showed an increase in the expression of anti-inflammatory cytokines IL-10 and a decreased expression of IL-6 compared to CIA+ mice (**Figure 1b)**. PET imaging at t28 and t56 confirmed that inflammation was only significantly reduced at the t56 timepoint (**Figure 1c**). Cellular studies at t28 and t56 showed increases T-regulatory cell populations in the spleen, inguinal lymph node (LN) and popliteal LN as determined by CD25 and FOXP3 expression (**not shown).** Histological analysis (H&E staining) of avacc treated mice showed decreased cellular infiltration and cartilage degradation in the synovium of the joints (**Figure 1d).**

Conclusions: These preliminary studies demonstrate that our engineered MP avacc formulation can (a) modulate the inflammatory environment in the paws of CIA mice towards anti-inflammation, (b) prevent the progression of collagen-induced arthritis. Herein, we show that this MP avacc is a potent biodegradable treatment option for CIA with tremendous potential for translation to use in humans.

References:
[1] Zhang W., Anis A.H. Clin Rheumatol, 2011. [2]Popov I., et al. Arthritic Research and Therapy, 2006 [3]Lewis, J.S., et al. Clin Immunol, 2015.

Environment-Responsive Two-Fluorophore Reporter System: A Potential Tool to Monitor Particulate Vomocytosis

Noah Pacifici[1], Amir Bolandparvaz[1], Shahin Shams[1], Roberta Stilhano[1,2], Eduardo Silva[1], and Jamal Lewis[1]
[1]UC Davis, Davis, CA, [2]Federal University of Sao Paulo, Sau Paulo, Brazil

Statement of Purpose: Pathogens have evolved over time to evade the host immune system in various ways. For instance, the fungal species *Cryptococcus neoformans*, following engulfment by phagocytes, has been observed to stay alive within the acidic phagolysosome and escape through a process called **vomocytosis**[1]. Using this phenomenon, *C. neoformans* utilizes host immune cells to disseminate infection throughout the body. One condition due to infection of this microbe is cryptococcal meningitis (CM). Primarily affecting immunocompromised individuals, including an estimated 220,000 HIV/AIDS patients, CM causes ~181,000 deaths/ year worldwide[2]. Greater understanding of vomocytosis could lead to the development of new CM treatments for patients, as well as novel biomaterial particulate vaccines. However, the underlying mechanisms of this phenomenon are unknown. To study vomocytosis, a method for quantifying phagocytosis and expulsion rates is required. Current studies use manual counting of vomocytic events[3] (**Fig. 1**) or multi-step flow cytometry staining[4] with limited success. **This work characterizes a novel dual fluorescent reporter system for precise monitoring of phagocytic entry and vomocytic expulsion**. The molecular signaling system is composed of tethered Enzyme-Labeled Fluorescence (ELF-97) and Fluorogen Activating Peptide (FAP). ELF-97 is a molecule that fluorescently activates upon cleavage by lysosomal phosphatases, indicating successful phagosomal uptake. The second indicator, FAP, is a protein that activates a cell-impermeable fluorogen (either αRED-np or MG Beta Tau) while outside of the cytoplasm and will be used to confirm escape from phagocytes. Here, poly(lactic-co-glycolic acid) (PLGA) microparticles (MPs) are used to demonstrate proof-of-concept for the transfer of the reporter system to *C. neoformans* and particulates.

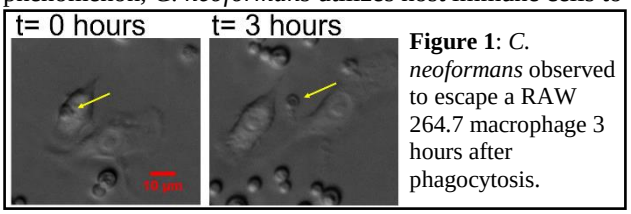

Figure 1: *C. neoformans* observed to escape a RAW 264.7 macrophage 3 hours after phagocytosis.

Materials and Methods: For this study, PLGA (50% PLGA + 50% PLGA-NH_2) MPs were synthesized using an oil/water emulsion. Dynamic light scattering (DLS) was used to size these particles as ~1µm. To create the dual reporter MPs, first ELF-97 was conjugated using EDC/imidazole chemistry (583µM ELF-97 in 1mg/ml MPs). Next, FAP (Silva Lab) was conjugated using an EDC/NHS linkage (5586nM FAP in 1mg/ml MPs). Reporter-conjugated *C. neoformans* were conjugated at identical concentrations. 2mg/ml phosphatase enzyme was used to activate the ELF-97. At least 1000nM was used to activate FAP. ELF-97 (Ex: 345nm, Em: 530nm) and FAP (Ex: 620nm, Em: 670nm) signals were detected via flow cytometry and fluorescent microscopy.

Results and Discussion: The reporter molecules ELF-97 and FAP successfully tethered to PLGA MPs, producing Reporter MPs**.** These particles were analyzed via flow cytometry for fluorescence under distinct activation prompts (**Fig. 2A**). On the Reporter MPs, ELF-97 fluorescence is detectable only after incubation with the phosphatase enzyme and FAP fluorescence is only activated upon exposure to the fluorogen. Reporter molecule conjugation was repeated but with the *C. neoformans* cell wall instead of PLGA MPs. Reporter-conjugated fungal cells successfully displayed fluorescent activation in phosphatase or fluorogen environments (**Fig. 2B**). To test the ability of conjugated ELF-97 to detect phagocytosis *in vitro*, RAW 264.7 macrophages were incubated with either ELF-97 MPs or blank MPs overnight; phagocytosed particles for each group were then imaged for ELF-97 signal, showing that ELF-97 particles strongly activate in the digestive phagolysosome (**Fig. 2C**).

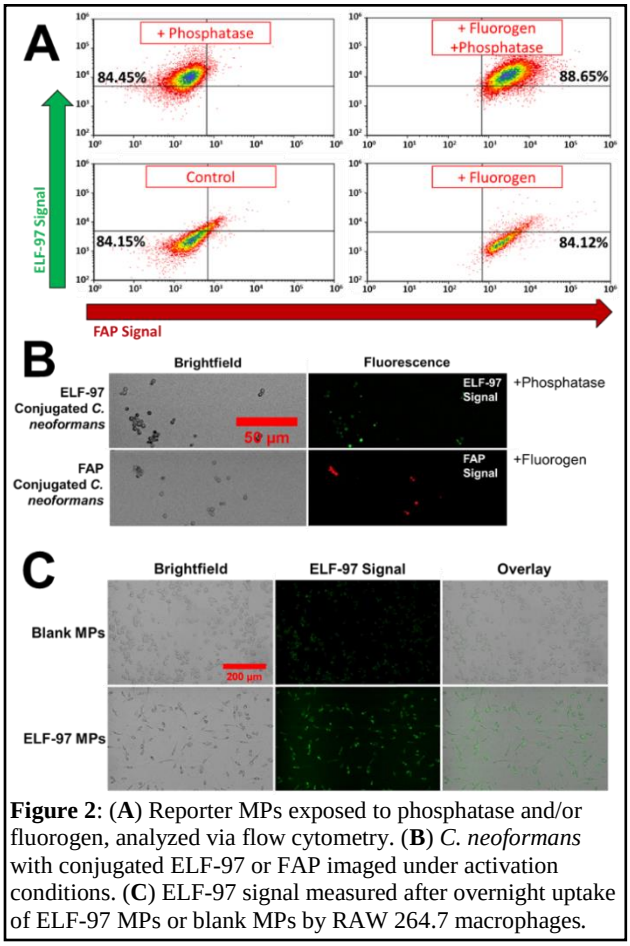

Figure 2: (**A**) Reporter MPs exposed to phosphatase and/or fluorogen, analyzed via flow cytometry. (**B**) *C. neoformans* with conjugated ELF-97 or FAP imaged under activation conditions. (**C**) ELF-97 signal measured after overnight uptake of ELF-97 MPs or blank MPs by RAW 264.7 macrophages.

Conclusions: These data demonstrate successful proof-of-concept for a dual-reporter system that shows robust fluorescent responsiveness to distinct activation prompts (phosphatase and fluorogen). This reporter system was shown to be conjugatable to both PLGA MPs and the *C. neoformans* surface. Furthermore, conjugated ELF-97 was shown to be activatable in the macrophage phagolysosome. Future work will involve investigation of FRET signal produced by these reporters. Next, this simple system will be used to monitor and measure vomocytosis *in vitro* and *in vivo* using reporter-conjugated *C. neoformans*.

Acknowledgements: NIH R35 Grant Funding, NIGMS-Funded Pharmacology Training Program (T32GM099608), NSF Graduate Research Fellowship

References: [1]Alvarez M. Curr Biol. 2006;16:2161-2165. [2]CDC [3]Gilbert AS. Sci Adv 2017;3(8):e1700898. [4]Nicola AM. MBio. 2011;2(4):e00167-11.

Towards a Nanoparticle-based Prophylactic for Maternal Autoantibody-related Autism

Amir Bolandparvaz[1], Rian Harriman[1], Natalia Vapniarsky[2], Kenneth Alvarez[1], Zexi Zang[1], Judy Van De Water[3], Jamal S Lewis[1]
[1]Department of Biomedical Engineering, University of California, Davis
[2]Department of Pathology Microbiology and Immunology, University of California, Davis
[3]M.I.N.D. (Medical Investigation of Neurodevelopmental Disorders) Institute, University of California, Davis

Introduction: Autism Spectrum Disorder (ASD) comprises a range of developmental disorders diagnosed in early childhood, where their ability to communicate and interact are impaired. In the U.S., an estimated 1 in 59 children[1] is born with ASD and the economic burden is a staggering $268 billion per year[2]. Current therapies are post-symptomatic and include behavioral interventions or symptom-derived pharmacological treatments. Recently, the Van De Water group discovered that about a quarter of ASD cases are caused by maternal autoantibodies (autoAbs) that can hinder normal neurodevelopment in the fetus. Moreover, they elucidated the seven proteins targeted by these autoAbs in the fetal brain, including lactate dehydrogenase A and B (LDHA, LDHB)[3]. Herein, we aim to develop a System for Nanoparticle-based Autoantibody Retention and Entrapment (SNARE) prophylactic as a biomagnetic trap - for sequestration of disease-propagating Maternal Autoantibody-Related (MAR) autoAbs. Our central hypothesis is that upon intravenous injection, the iron oxide NPs surface-conjugated with autoantigens will circulate throughout the maternal vasculature, and specifically ligate MAR autoAbs, thereby limiting antibody (Ab) transport across the placenta and preventing MAR autism. Currently, investigative aims are to synthesize SNAREs, assess Ab binding capacity, cytotoxicity and immunogenicity *in vitro*, as well as determine *in vivo* distribution and maximum tolerated dose.

Materials and Methods: We synthesized magnetite dextran iron oxide NPs (DIONPs) by a standard co-precipitation method with dextran (MW 10 kDa) and surface-modified with citric acid (CA) and methoxy poly(ethylene glycol) (PEG) amine via EDC chemistry. We performed physico-chemical characterization of the DIONPs with TEM, DLS, FTIR, TGA, and a zeta potential assay (not shown). Furthermore, DIONPs were surface-conjugated with FITC-LDH B (15 amino acids) peptide via EDC reaction (finalized formulation referred to as SNAREs) (not shown). Notably, LDH B Ab capture was demonstrated by incubating SNAREs with serum from mothers of children with autism and then assessing the LDH B Ab serum titer after separation of the SNAREs. Further, we assessed cytotoxicity on RAW264.7 macrophages, immunogenicity (not shown), and NP cellular uptake by Prussian Blue iron stain. *In vivo,* we investigated the maximum tolerated dose (MTD) by tail vein injection of (0.1-10)*LC25 SNARE dose on Gestation Day 12 in C57/BL6 pregnant mice. Post-mortem necropsy of fetuses and dams assessed for toxicity by a complete blood count, serum composition, hematological and histological analysis of major organs (not shown), and Prussian Blue stain of histological slides to determine distribution.

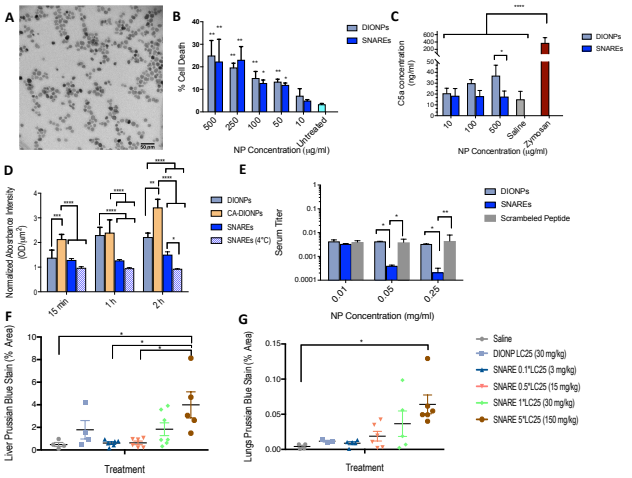

Fig 1: A. TEM of DIONPs **B.** RAW264.7 macrophage cell viability in presence of NPs (DIONPs or SNAREs) **C.** Complement activation in mouse serum in presence of NPs **D.** Phagocytic uptake of NPs by macrophages **E.** *In vitro* LDH B antibody capture by NPs in patient-derived serum **F-G.** Deposition of SNAREs in the liver and lungs of pregnant dams. P<.05(*), P<.01(**), P<.001 (***), P<.0001 (****).

Results and Discussion: Based on TEM analysis and DLS measurements, the unmodified DIONPs demonstrate desired size and shape of ~15 nm in diameter (Fig 1: A). FITC-LDH B peptide conjugation to PEGylated DIONPs was quantified at 33.8 μg peptide/cm^2 DIONP and 70% efficient (not shown). SNARE cytotoxicity on macrophage cells for 25% lethal concentration (LC25) dose was at ~500 μg/ml (Fig 1: B). Further, SNAREs interaction with serum did not significantly elevate C5a complement fragment concentration (Fig 1: C). Nanoparticle uptake by macrophages at 1 h and 2 h incubation times demonstrated significantly lower uptake of SNAREs vs CA-DIONPs and DIONPs (Fig 1: D). Also, DIONPs and SNAREs demonstrated no significant activation of bone-marrow derived macrophages or dendritic cells. Remarkably, LDH B Ab titer in patient-derived human serum was reduced by 90% by exposure to SNAREs (0.25 mg/ml) (Fig 1: E). *In vivo*, tail vein injection of SNAREs and DIONPs demonstrated significant NP accumulation in liver and lungs at the highest administered dose (150 mg NPs/kg) (Fig 1: F-G). However, mice displayed no overt signs of distress, maternal or fetal toxicity at this dosage indicating that this may be the MTD dose for the SNAREs.

Conclusion: These preliminary studies demonstrate that we can surface functionalize DIONPs with PEG and MAR LDH B peptide and use this formulation to *capture LDH B autoantibodies from serum*. This nanotechnology has the potential to be the very first prophylactic for autism. Future studies will include (a) SNARE optimization (b) assessing *in vivo* clearance via MRI in pregnant mice, and (c) efficacy in a MAR autism mice model.

References: 1. Baio 2018; MMWR Surveill Sum **2.** Leigh, 2015; J Autism Dev. Disorder **3.** Braunschweig, 2012 Neur Rev